

Review

Modeling the Succinic Acid Bioprocess: A Review

Itziar A. Escanciano ¹, Mateusz Wojtusik ¹, Jesús Esteban ², Miguel Ladero ^{1,*} and Victoria E. Santos ¹

¹ FQPIMA Group, Department of Chemical Engineering and Materials, Faculty of Chemistry, Complutense University of Madrid, 28040 Madrid, Spain; itziaria@ucm.es (I.A.E.); mwojtusik@ucm.es (M.W.); vesantos@ucm.es (V.E.S.)

² Department of Chemical Engineering and Analytical Science, University of Manchester, Manchester 46962, UK; jesus.estebanserrano@manchester.ac.uk

* Correspondence: mladerog@ucm.es

Abstract: Succinic acid has attracted much interest as a key platform chemical that can be obtained in high titers from biomass through sustainable fermentation processes, thus boosting the bioeconomy as a critical production strategy for the future. After several years of development of the production of succinic acid, many studies on lab or pilot scale production have been reported. The relevant experimental data reveal underlying physical and chemical dynamic phenomena. To take advantage of this vast, but disperse, kinetic information, a number of mathematical kinetic models of the unstructured non-segregated type have been proposed in the first place. These relatively simple models feature critical aspects of interest for the design, control, optimization and operation of this key bioprocess. This review includes a detailed description of the phenomena involved in the bioprocesses and how they reflect on the most important and recent models based on macroscopic and metabolic chemical kinetics, and in some cases even coupling mass transport.

Keywords: succinic acid; fermentation; kinetic model; mass transport; phenomenology; carbon dioxide



Citation: Escanciano, I.A.; Wojtusik, M.; Esteban, J.; Ladero, M.; Santos, V.E. Modeling the Succinic Acid Bioprocess: A Review. *Fermentation* **2022**, *8*, 368. <https://doi.org/10.3390/fermentation8080368>

Academic Editor: Silvia Greses

Received: 8 June 2022

Accepted: 29 July 2022

Published: 31 July 2022

Publisher's Note: MDPI stays neutral with regard to jurisdictional claims in published maps and institutional affiliations.



Copyright: © 2022 by the authors. Licensee MDPI, Basel, Switzerland. This article is an open access article distributed under the terms and conditions of the Creative Commons Attribution (CC BY) license (<https://creativecommons.org/licenses/by/4.0/>).

1. Introduction

The world gross domestic product (GDP) has been almost quintupled in the last 60 years due to intense global growth and the ever-growing search for the welfare state [1]. In this global scenario, the use of fossil fuels has grown at unprecedented rates. In fact, fossil fuel subsidies remained at USD 5.9 trillion in 2020, which represents 6.8% percent of the global GDP of that year [2]. At the current consumption rates, it is expected that only 14% of the present oil reserves, 72% of coal reserves and 18% of gas reserves will remain by 2050 [3,4]. In addition to the scarcity of these resources, the pernicious impact on health and the environment of the regular utilization of fossil fuels must be taken into account [5–8].

As a logical consequence of the aforementioned issues and owing to a scenario of growing social concern for health and the environment, there has been a remarkable boost in research efforts towards the implementation of integrated biorefineries (IB). Their objective is the efficient use of biomass as a raw material for the production of biofuels, energy and chemicals in a single integrated facility [9,10]. Among the different IB types, those using lignocellulosic biomass as feedstock can be highlighted. Amidst their main advantages are the transformation of a wide variety of low-cost raw materials including, e.g., straw, reed, pruning . . . as well as the ability to obtain highly demanded products in markets currently covered by petrochemicals, with the prospects of opening new markets by producing further chemicals by organic synthesis [9–11].

One of the main challenges to overcome in biorefineries is the use of a type of biomass with long-term availability. Considering that biomass is any organic resource derived from plants or animals, we can count on lignocellulosic biomass, algal biomass, biomass from food waste and industry or even municipal solid waste [12]. Lignocellulosic biomass is the most abundant renewable resource in the biosphere [13] and since it does not interfere

in any food chain, this raw material is especially attractive in biorefinery processes [14]. It is generated by the photosynthesis process: the combination of CO₂ and H₂O using ultraviolet radiation from sunlight as an energy source results in sugars as the primary products with the subsequent production of O₂ as a by-product [15,16]. Lignocellulosic material consists of plant tissues whose cells have a wall made up of a network of cellulose microfibrils that group into larger fibers linked by hemicellulose. The structural integrity of these microfibrils is protected by the presence of lignin, which acts as a linker [17,18].

However, the recalcitrance of lignocellulosic biomass demands on severe physical, chemical, physicochemical and biological pretreatments to leave the final solids accessible and reactive, thus rendering them available for hydrolysis into C5 and C6 monosaccharides. In consequence, these processes face several challenges to achieve high efficiencies and conversion yields without compromising their sustainability and cost-effectiveness [19,20].

Succinic acid (SA) is a key platform chemical for the bioeconomy due to the reactivity of its two functional carboxylic groups, which allows for obtaining a wide range of end-products [20,21]. In fact, according to the United States Department of Energy (US DOE), this compound is one of the target molecules that could be produced from biorefinery carbohydrates and from which many other products of interest may arise [22,23]. In fact, SA is considered the most important C4 building block and is widely used in several industries [24–26]

Since it has been demonstrated that SA has a positive influence on human metabolism, without the risk of bioaccumulation, it has been used in the food industry as an acidulant, flavoring agent and sweetener [27]. Moreover, in the traditional chemical industry, this compound has been key to the synthesis of other notable products, such as polybutylene succinate and polybutylene succinate-terephthalate, polyester or polyols, as well as in the pharmaceutical industry and in the production of resins, coatings and pigments. In addition, as the paradigm shift towards a bioeconomy evolves and becomes more and more established, SA has an outstanding potential for the generation of many intermediate chemicals of industrial relevance, such as 1,4-butanediol, butyriol-butone, tetrahydrofuran, n-methyl-2-pyrrolidone, 2-pyrrolidone, succinimide or maleic acid/maleic anhydride. Furthermore, succinate and its derivatives could be used for the manufacture of biodegradable polymers as polyamides and polyesters [19,21,28–30]. Figure 1 illustrates a diagram compiling the main products that can be obtained from SA.

Traditionally, the production of SA has been carried out through chemical technologies such as the oxidation of paraffins or the catalytic hydrogenation of maleic acid or maleic anhydride [21,27,31,32].

Microbial production of SA could become competitive due to several advantages, such as a high yield of SA from the conversion of carbon content or a significant reduction in greenhouse gas emissions and non-renewable energy consumption. Furthermore, a large amount of CO₂ is fixed during the process, which adds to the potential of this process as a mitigating strategy in the production of a commodity chemical [21,33].

Currently, the biotechnological production of SA prevails in the market compared to other routes. In 2011, the bioproduction of this compound accounted for less than 5% of the total production; however, only six years later, this share increased to practically 49% [34]. This increasing trend is expected to continue, predictably reaching a market volume of SA biotechnological production worth USD 2.22 billion by 2026, in contrast with the USD 170 million value in 2020 [35]. In realization of the expanding market for this product and the advantages offered by the biological production of SA, numerous companies have invested in the construction of industrial facilities for the production through this route. The production of this compound at an industrial level is especially advanced in Europe and North America, where its technological readiness level (TRL) is eight, which in turn means that there are complete and certified systems through tests and demonstrations [21]. In 2015, succinic acid produced by bioprocesses had a market price of USD 2.86 per kg, while if it was obtained from fossil sources the price was around to USD 2.5 per kg [34]; however, as greenhouse gas emissions more than double during petrochemical production and the

raw material costs are also higher (and their future availability uncertain), researchers and companies are increasingly turning to sustainable biological processes [21]. Currently, it has been possible to develop some economically competitive succinic acid production processes, with the acid produced having a market price between 2 and 2.5 USD kg⁻¹ [36].

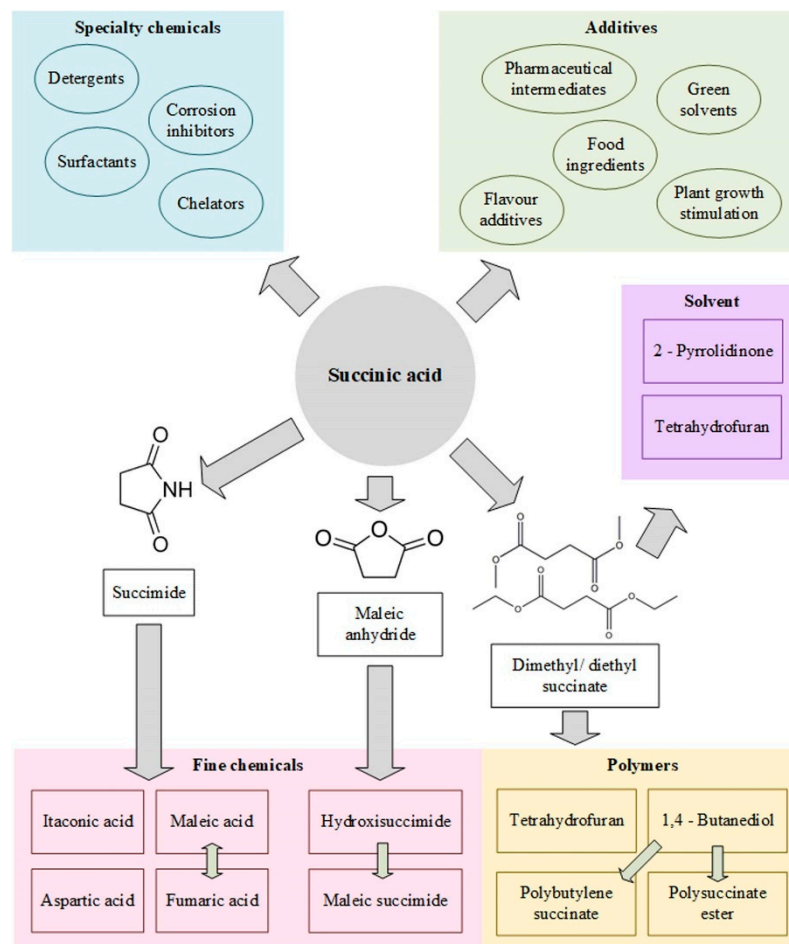


Figure 1. Array of intermediate and end products stemming from succinic acid.

1.1. Succinic Acid Bioproduction

According to the literature, the production of succinic acid is usually carried out between 33 and 39 °C at a controlled pH between 6.5 and 7. CO₂ is usually supplied to the system by insufflation in a gaseous state or by incorporating carbonates into the system, with MgCO₃ leading to the best production yields [19,37–44]. Most biological processes depend usually on the reaction or residence time (depending on the use of batch, fed-batch or continuous operating bioreactors); therefore, researchers have experimented with different configurations and types of reactors, managing to increase yields considerably with repeated batch and fed batch operating bioreactors [45–47]. In addition, continuous operation with a biofilm formation, in some cases, has resulted in highly improved productivities [48–51].

Almost all microbial, plant, and animal cells can generate SA; however, throughout the years it has been observed that the most suitable organisms for the production of this compound are fungi and bacteria [27]. Some fungi such as *Aspergillus niger*, *Penicillium viniferum*, *Yarrowia lipolytica*, and the yeast, *Saccharomyces cerevisiae*, generate SA as a by-product of their metabolism in aerobic and/or anaerobic conditions [21,52]. The most investigated bacterial strains are *Actinobacillus succinogenes*, *Anaerobiospirillum succiniciproducens*, recombinant *Escherichia coli*, *Corynebacterium glutamicum* and *Mannheimia succiniciproducens*, [29,52–55]. Being the isolates from the rumen (*A. succinogenes* and *M. succiniciproducens*), they are

the ones that could obtain the most promising results, since they naturally generate C4 dicarboxylic acids during the pregastric digestion of polysaccharides. [25,29,52,56].

The latter microorganisms produce SA via the so-called tricarboxylic acid cycle (TCA), a cycle depicted in Figure 2. After sugars have been transformed into glyceraldehyde, bacteria convert phosphoenolpyruvate (PEP) (the last product of glycolysis) into oxalacetic acid, requiring CO₂ to activate this metabolic pathway. Oxalacetate is subsequently reduced in a series of steps until SA is produced [29,36]. From the reaction pathway showing in TCA, theoretically, to obtain 1 mol of SA, 2 moles of reduced nicotinamide adenine dinucleotide (NADH) and 1 mol of CO₂ would be necessary. As for sugars, 0.5 mol of glucose, 0.6 mol of xylose or 1 mol of glycerol would be necessary to generate another mol of succinate [26].

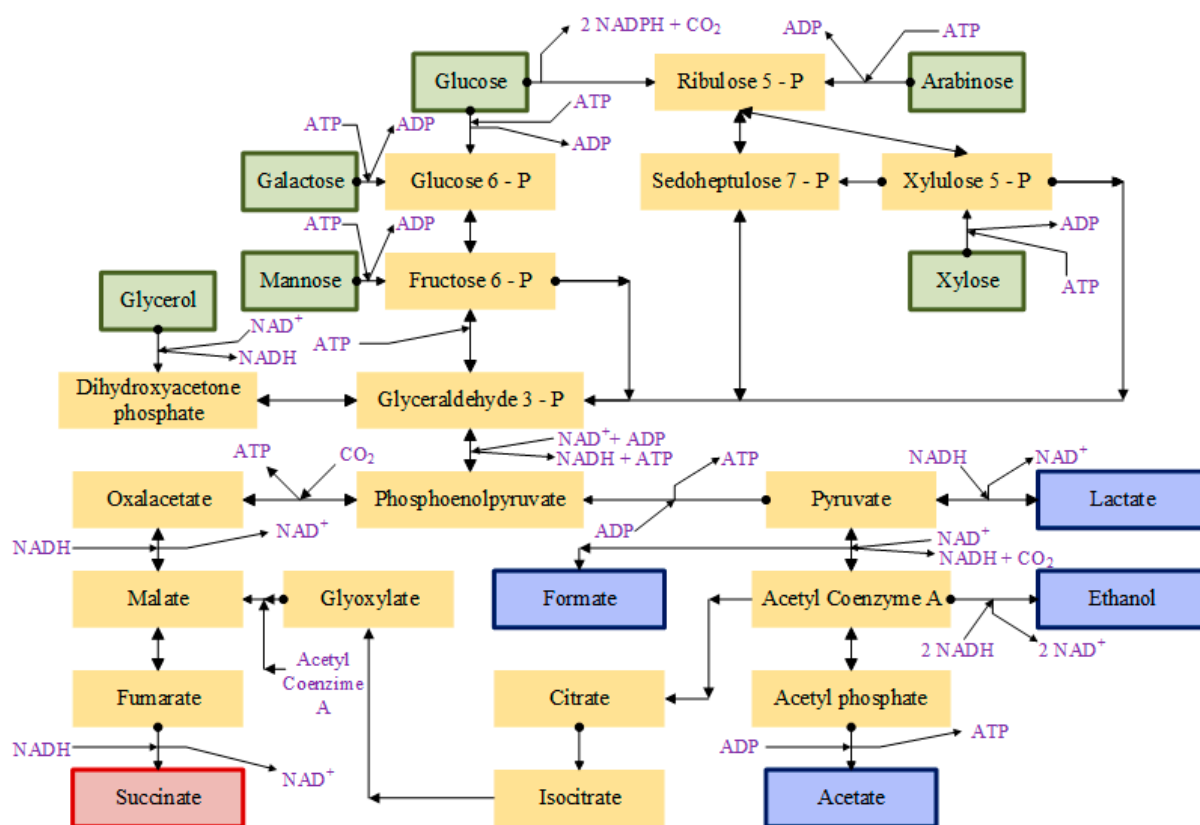


Figure 2. Metabolic pathways in succinic acid-producing microorganisms such as *A. succinogenes*, *A. succinoproducens*, *M. succiniproducens* and anaerobic succinate engineered *E. coli*. [26,28,29], Adenosine triphosphate (ATP), flavin adenine dinucleotide (FAD⁺), nicotinamide adenine dinucleotide (NAD⁺), reduced nicotinamide adenine dinucleotide (NADH), and reduced nicotinamide adenine dinucleotide phosphate (NADPH).

It is very important to highlight the different physiological features of SA-producing bacteria. *A. succinoproducens*, *A. succinogenes* and *M. succiniproducens* naturally produce SA as the main product of fermentation in the presence of CO₂ via the PEP carboxylase pathway [26,28]. It has been found that in the metabolism of *A. succinoproducens*, PEP carboxylase (PEPCK) is the main CO₂-fixing enzyme for the generation of oxaloacetate. Furthermore, the conversion of pyruvate to acetyl-CoA is dependent on pyruvate-ferredoxin oxidoreductase; therefore, the control of pH and CO₂ concentration are critical in fermentations with *A. succinoproducens*, since PEPCK and pyruvate-ferredoxin oxidoreductase are strongly dependent on these parameters. Their optimization would lead to an increase in the productivity of succinic acid and a reduction in the generation of by-products (lactic acid, acetic acid and ethanol) [28,54]. *A. succinogenes* and *M. succiniproducens* have many aspects of their metabolism in common. In both cases, the main fermentation products are succinate, acetate and formate; however, the first of them can also generate ethanol,

while the second would produce lactic acid. In its metabolism, oxalacetic acid is formed thanks to the action of PEPCK and is subsequently reduced to succinate by the C4 pathway. Although it is probably not the main enzyme in this process, it has been suggested that *M. succiniproducens* can also use PEP carboxylase (PEPC) for the carboxylation of oxalacetic acid [26]; however, PEPC is not encoded in the *A. succinogenes* genome. Succinic production does not take place simply due to part of the PEP branching to the C4 pathway. This must be taken into account since the increase in CO₂ concentration decreases the C4 decarboxylation flux, increases the pyruvate carboxylation flux and barely affects the PEPCK [26,28,54]. Although *E. coli* is capable of producing succinic acid through the reducing branch of tricarboxylic acid (TCA), it is not the main product of its fermentation naturally, which is why metabolic engineering has been used to increase production [26,29]. PEP, PEPC, and pyruvate-carboxylating enzymes have been overproduced to direct metabolic flux to the TCA-reducing branch. *A. succinogenes* PEPCK, pyruvate carboxylase (PYC) from *Lactococcus lactis* or *Rhizobium etli* have also been overproduced [26]. The *E. coli* NZN11 strain is capable of excreting pyruvate by increasing its carboxylation; however, it is not capable of fermentative growth and when malic enzyme is overproduced, the succinic production is greatly slowed down. [26,54]. Thanks to experiments on the transition from the aerobic growth phase to anaerobic production carried out with *E. coli*, it was discovered that, during aerobic growth, a new pathway was activated that involved the derivation of glyoxylate, using less reducing power and complementing the reducing branch of TCA [26]. With the AFP111 and SBS550MG/pHL413 strains, the aim was to eliminate the fermentation by-products and guarantee the glyoxylate bypass flow; however, it must be taken into account that if an additional reductant could be used, the glyoxylate route would be less efficient than in the case of maximizing the flow of the reductant TCA branch. *C. glutamicum* in anoxic conditions, with carbonate and when growth is absent, is capable of producing succinic, lactic and acetic acids. In this microorganism, oxalacetic acid is produced mainly thanks to the action of PEPC with less contributions from PEPCK and PYC, later this compound gives rise to succinic acid through the reductive branch of the TCA cycle, not being necessary the glyoxylate shunt [26,54].

1.2. The Importance of Kinetic Modeling

In light of the relevance of SA in the context of biorefineries and how these will become a trend spurred by global policies, this review intends to provide an extensive overview of empirical models that describe its biotechnological production. The formulation of models capable of describing the evolution of the compounds involved in fermentation is of great importance in the industrialization of biotechnological processes. These models allow the simulating of the temporal behavior of the system, which, from an engineering point of view, is essential for the development and scale-up of the process. Taking into account that the performance and productivity of a process not only depend on the genetic constitution of cells, but also on the way in which fermentation is carried out, these models are especially useful for the choice of the reactor and its design. Furthermore, these models can also be implemented in the design a control system, and will definitely aid during scale-up and industrial process simulation and implementation through diverse techno-economic studies. In fact, a mathematical description of the process, typical in process systems engineering [57], allows its optimization through simulation, saving time, effort and resources for experimentation at several scales. As a consequence, differential equations are established for the rates at which biochemical reactions are taking place. This set of equations are usually called kinetic models, although they are also called dynamic models, due to the overlapping of concepts in terms of biological models [58–60].

Therefore, to conduct fermentation processes at an industrial level implies the consideration of different amounts of materials and energy inputs at each production level, which can affect the behavior of the microorganism; therefore, it is necessary to approach an isolated study of different individual phenomena and variables on a laboratory scale prior to their simultaneous consideration. In this way, proper coupling of the phenomena

can then accurately describe the overall process [60,61], as shown in Figure 3, from the point of view and language of chemical reaction engineering.

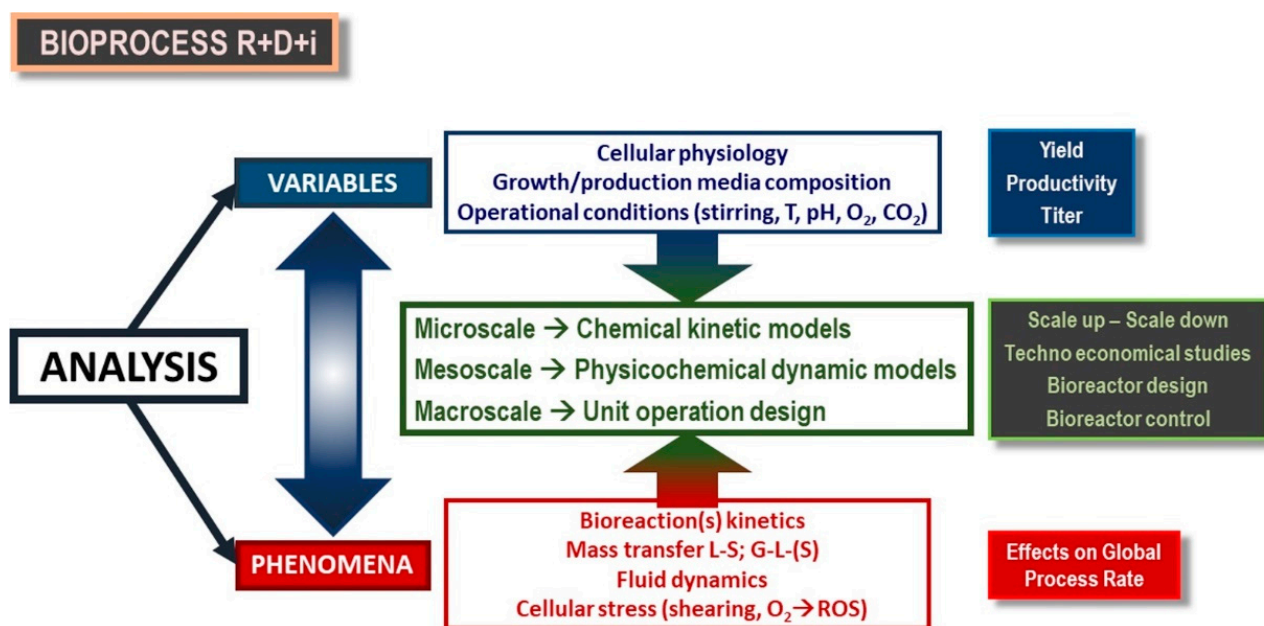


Figure 3. Dynamic phenomena coupling and modelling in a research, development and innovation (R+D+i) scheme for the implementation of a bioprocess.

The major dynamic phenomena to take into account are the following:

- Mass transfer among phases. Due to the fact that microbial systems for the production of succinic acid are heterogeneous (gas–liquid–solid), it is essential to study the transport of nutrients among phases in the system [29,36,41,42].
- Reaction kinetics in the system. The description of a bacterial reaction network is very complex, although the evolution of the concentrations can be described through a kinetic model [62].
- Stress suffered by the cells. Due to the hydrodynamic conditions and the presence of radical species (ROS) and other operational parameters, the physiology of the cells may undergo severe changes throughout the bioprocess, which may be deleterious to their performance [58,61–63].

2. Kinetic Models

Through microbial kinetics, the manifestations and reactions of microbial life can be studied, namely, growth, survival, death, adaptations, product formation, cell cycles and interactions with the environment; therefore, to determine the economic loss or gain of the processes, it is essential to establish models that represent their kinetic behavior. The formulation of the kinetic model consists of the approach of a simplified network of reactions that describes the lumped chemical transformations that take place as well as the kinetic equations that determine the rate at which each of the reactions involved in the network takes place. The proposed kinetic equations are differential equations that can derive from phenomenological hypotheses or empirical descriptions. From the reaction scheme and the reaction rates, the production rate of each compound is proposed, taking into account the reactions in which each one is involved and their stoichiometry. The complexity of the study of biochemical metabolism lies in the network of reactions that take place, since routes are distinguished both for the synthesis of complex molecules and the precursors of intermediates (anabolic route) and for the supply of the necessary energy in the anabolic processes (catabolic routes). Such models can have different degrees of complexity and provide different extents insights into the underlying phenomena; thus,

they can take the shape of correlations that range from purely empirical (black box) to fully mechanistic (white box) ones. In any case, they help establish relationships between the reaction rates and concentrations of the species inserted in material balances and allow the prediction of conversion degrees and yields [62].

Due to its simplicity, currently, the most widespread models are those that consider the microorganism as a single component (biomass), in other words, the so-called unstructured-non-segregated models; however, there are other more complex models. In metabolic models, although they are also normally unstructured-non-segregated, the metabolic pathways are described as a network of reactions using a simplified reaction scheme, with defined stoichiometric relationships. When the description of biomass is made considering it to be made up of several species, taking into account the intracellular components, it is a structured model (or cell model). The chemically structured models consider the biomass formed by several species and also a simplified metabolism (a network of reactions). The segregated models describe the microorganism considering the distribution of some property, that is, they do not consider an average microorganism but diverse microbial populations [58,64,65].

Numerous research efforts have focused on studying the kinetic evolutions of the compounds involved in the SA production process using different microorganisms. This has allowed conclusions to be drawn on general growth trends and inhibitory behaviors. From the performance of fermentations operating in batch, repeated batch and fed batch modes, it has been possible to observe how the SA-producing microorganisms show certain behaviors in the consumption of substrates and the generation of products and by-products [38,66,67].

Comparing the time evolution of SA together with the trend of biomass, it can be observed that, regardless of the microorganism or substrate used [67–72], the main product begins to generate before the biomass reaches the steady state. Moreover, the product concentration continues to grow during the stationary phase of the microorganism; therefore, it can be deduced that the production of SA is partially associated with the growth of biomass.

It is known that some compounds present in the hydrolysates of lignocellulosic raw materials, such as furfural, hydroxymethylfurfural or phenolic compounds, act as inhibitors; therefore, their concentrations in the culture broth are factors that must be taken into account when studying the kinetics of the process [19,73,74]. However, other factors that may affect the activity of the microorganisms, and, therefore, the kinetic models and their parameters, must also be considered. It is necessary to maintain adequate pH levels, whose optimal value is usually considered to be 6.8. Another variable to take into account is the nature of the compound used as a regulator. Under anaerobic conditions, it has been observed that the replacement of typical hydroxides (KOH, NaOH) by carbonates (K_2CO_3 , Na_2CO_3 , $MgCO_3$) leads to higher cell viability and, therefore, to a higher final concentration of SA [75,76]. Furthermore, $MgCO_3$ can also act as a source of CO_2 , and the infusion of this gas can be totally or partially substituted, maintaining the yields or even exceeding them [76]. Osmolarity has also proven to influence the SA production process, but its effects can be considered negligible compared to those generated by organic acids in the medium such as SA, FA, AA and PA [38,39,70,77,78]. Inhibitions by substrates must also be considered, since it has been verified that both high concentrations of glucose [38,77,79] and xylose [39,80] generate this effect.

2.1. Non-Segregated, Unstructured Models

Non-segregated unstructured models are the most widely used in chemical engineering. Depending on the variables they consider, a wide variety of them with different degrees of complexity can be distinguished [60].

2.1.1. Biomass Growth Models

First, there are the models that consider biomass concentration as the only determining factor for its growth. The most representative equations are Malthus' Law for the exponential phase in steady state systems—Equation (1) and the logistic equation—Equation (2)—[81]:

$$\frac{d[X]}{dt} = \mu \times [X] \tag{1}$$

$$\frac{d[X]}{dt} = \mu \cdot [X] \times \left(1 - \frac{[X]}{[X]_m} \right) \tag{2}$$

where $[X]$ is the biomass concentration, t is time, μ is the specific growth rate and $[X]_m$ is the maximum biomass concentration.

Another type of equation is presented in Equation (3), in which the growth of biomass is dependent on the concentration of biomass and the limiting substrate ($[S]$), the latter dependence being included in the specific growth rate:

$$\frac{d[X]}{dt} = \mu([S]) \times [X] \tag{3}$$

Blackman, M'Kendric and Pai and Tessier proposed expressions for the calculation of the specific growth rate considering the influence of the limiting substrate: however, the Monod model—Equation (4)—is considered a fundamental equation in microbial kinetics and is also the most widely used for the description of biomass in the production of SA [39,78,82]. This empirical model is an analogy to the Michaelis Menten model for unisubstrate irreversible enzymatic reactions and is based on the enzymatic nature of the reactions that take place inside the microorganism [39,61]:

$$\mu = \frac{\mu_m \times [S]}{K_S + [S]} \tag{4}$$

In this equation, μ_m is the maximum specific growth rate and K_S is the saturation constant of the substrate.

Deriving from this model, numerous expressions have been developed to describe the growth of biomass considering the inhibition by substrate. The main expressions that have been used for the modelling of SA generation experiments are shown below—Equations (5)–(12)—which derive either by a combination of some of them [38,40,83] or by application in their original form [56,82,84]:

| | | |
|--------|--|-----|
| Mosser | $\mu = \frac{\mu_m \times [S]^n}{K_S + [S]^n}$ | (5) |
|--------|--|-----|

| | | |
|---------|---|-----|
| Tessier | $\mu = \mu_m \times \left(1 - e^{[S]/K_S} \right)$ | (6) |
|---------|---|-----|

| | | |
|--------------------|--|-----|
| Tessier (high [S]) | $\mu = \mu_m \times \left(e^{-[S]/K_{IS}} - e^{-[S]/K_S} \right)$ | (7) |
|--------------------|--|-----|

| | | |
|-----------------|--|-----|
| Haldane–Andrews | $\mu = \frac{\mu_m \times [S]}{[S] + K_S + \left(\frac{[S]^2}{K_{IS}} \right)}$ | (8) |
|-----------------|--|-----|

| | | |
|--------------------|---|-----|
| Andrews (high [S]) | $\mu = \frac{\mu_m}{\left(1 + \frac{K_S}{[S]} \right) \times \left(1 + \frac{[S]}{K_{IS}} \right)}$ | (9) |
|--------------------|---|-----|

| | | |
|-------------|--|------|
| Aiba–Edward | $\mu = \frac{\mu_m \times [S]}{[S] + K_S} e^{-[S]/K_{IS}}$ | (10) |
|-------------|--|------|

| | | |
|-------|--|------|
| Luong | $\mu = \frac{\mu_m \times [S]}{[S] + K_S} \cdot \left(1 - \frac{[S]}{[S]_m} \right)^\alpha$ | (11) |
|-------|--|------|

| | | |
|--------------|---|------|
| Jerusalimsky | $\mu = \mu_m \left(\frac{1}{1 + [S]/K_{IS}} \right)$ | (12) |
|--------------|---|------|

In these equations, n indicates the degree of inhibition ($n = 1$ in the Monod model), K_{IS} is the inhibition constant per substrate and α is a parameter relating μ and $[S]$.

Since the inhibition by product also occurs during fermentation, other models have been developed to take this phenomenon into account. When this is the case, the specific growth rate can be expressed by Equation (13):

$$\mu = \frac{\mu_i \times [S]}{K_S + [S]} \tag{13}$$

where μ_i is the maximum specific growth rate in the presence of an inhibitor. In studies of the kinetics of SA generation [41,56,79,85], the main expressions used are those corresponding to Equations (14) to (16):

$$\text{Luong} \quad \mu_i = \mu_m \times \left(1 - \frac{[P]}{[P]_m}\right)^\beta \tag{14}$$

$$\text{Aiba-Edward} \quad \mu_i = \mu_m \times e^{-[P]/K_{IP}} \tag{15}$$

$$\text{Jerusalimsky} \quad \mu_i = \mu_m \times \left(\frac{1}{1 + [P]/K_{IP}}\right) \tag{16}$$

in which $[P]$ is the product concentration, β is the reaction between μ and $[P]$ and K_{IP} is the inhibition constant per product.

2.1.2. Substrate Consumption Models

Equation (17) shows the simplest expression for obtaining the rate of substrate consumption. It is based on the relationship between the coefficient of yield of substrate in biomass (Y_{SX}) and the specific growth rate, and is one of the most used in the kinetic study of the production of SA.

$$\frac{d[S]}{dt} = \mu \times Y_{SX} \tag{17}$$

However, several researchers have considered that the substrate is also consumed to maintain biomass in a viable state throughout the reaction. For this reason, they have introduced the so-called Pirt’s maintenance coefficient m [38,40,83,86] in the substrate consumption equations. Furthermore, some of these authors have also included a term in their models that allows for describing the consumption of energy substrate for production [38,83,86], as shown in Equations (18) and (19):

$$\frac{d[S]}{dt} = \left(-\frac{1}{Y_{XS}} + \sum_I \frac{1}{Y_{PiS}}\right) \times \frac{d[X]}{dt} + \left(-\sum_I \frac{1}{Y_{PiS}} + m\right) \times [X] \tag{18}$$

$$\frac{d[S]}{dt} = \left(-\frac{1}{Y_{XS}}\right) \times \frac{d[X]}{dt} + \left(-\sum_i \frac{1}{Y_{PiS}}\right) \frac{dP_i}{dt} + (-m) \times [X] \tag{19}$$

2.1.3. Product Generation Models

Most kinetic studies on the biological production of SA predict the generation rate of this compound and of the by-products through the Luedeking–Piret expression—Equation (20)—as is logical in a production process partially affected by the growth of the biomass [38,83,86,87].

$$\frac{d[P_i]}{dt} = \alpha_i \times \frac{d[X]}{dt} + \beta_i \times [X] \tag{20}$$

where $[P_i]$ is the concentration of SA or by-product, α_i is the associated growth parameter and β_i is the non-associated growth parameter; however, in some cases simpler expressions have been used, such as the one used in Equation (21), where the generation of SA only depends on the specific growth rate [88]. In other instances, expressions of greater complexity have been regarded, such as the modified Gompertz model [89] as seen in

Equation (22), where $[P_m]$ is the maximum metabolite concentration, R_m is the maximum rate of metabolite production, e is the Euler number and λ is the time of the latency phase.

$$\frac{d[P]}{dt} = \mu \times Y_{PX} \tag{21}$$

$$[P] = [P_m] \times \exp\left(-\exp\left[\frac{R_m \times e}{[P_m]}(\lambda - t) + 1\right]\right) \tag{22}$$

For experimental data obtained in continuous processes, relatively simple empirical expressions have been proposed to describe SA production [85]. On the other hand, Ferone et al. proposed Equation (23) [90], where the variation of the concentration of SA is represented as a function of the dilution rate (D). Under steady state conditions, D is equivalent to the specific growth rate.

$$\frac{d[P]}{dt} = \frac{D \times [P]}{[X]} \tag{23}$$

Table 1 presents a summarized compilation and classification of kinetic studies carried out on the bioproduction of SA in recent years, in which non-segregated unstructured models are proposed and fitted to experimental data.

Table 1. Non-segregated unstructured kinetic models.

| Microorganism | Operation Mode | Carbon Source | Species Predicted by the Model | | | | Ref. |
|---|------------------|--|--|---------------|---------------|---------------|------|
| | | | Biomass | Substrate | Product | By-Products | |
| <i>A. succinogenes</i> 130Z, <i>E. coli</i> NZN111, AFP111, BL21 | Batch | Glucose | Equations (1), (2) | | | | [78] |
| <i>A. succinogenes</i> DSM 22257 | Batch | Glucose, mannose, xylose, arabinose | Equations (1), (4), (8) | | | | [39] |
| <i>E. coli</i> ATCC 8739 | Batch | Glycerol | Equations (1), (4)–(10) | | | | [82] |
| <i>B. succiniciproducens</i> BPP7 | Fed Batch | <i>Arundo Donax</i> hydrolysate | Equations (1), (14) | | | | [41] |
| <i>A. succinogenes</i> 130Z | Batch | Glucose | Combination of Equations (1), (12), (16) | Equation (17) | | | [79] |
| <i>A. succinogenes</i> DSM 22257 | Continuous | Glucose | Combinations of Equations (1), (4), (8), (11), (14)–(16) | | Equation (23) | | [90] |
| <i>A. succinogenes</i> 130Z | Batch | Oil palm frond hydrolysate | Equation (8) | | Equation (22) | | [89] |
| <i>A. succinogenes</i> 130Z | Continuous | Glucose | Empirical | | Empirical | | [85] |
| <i>A. succinogenes</i> 130Z | Batch, Fed Batch | Raw carob pod extracts | Equations (1), (4) | Equation (17) | Equation (20) | | [87] |
| <i>A. succinogenes</i> ATCC 55618 | Batch | Glucose | Combination of Equations (1), (11), (14) | Equation (18) | Equation (20) | Equation (20) | [38] |
| <i>A. succinogenes</i> ATCC 55618 | Batch | Glycerol | Combination of Equations (1), (8), (14) | Equation (19) | Equation (20) | Equation (20) | [86] |
| <i>A. succinogenes</i> 130Z, <i>B. succiniciproducens</i> JF 4016 | Batch | Xylose, galactose, glucose, mannose, arabinose | Combination of Equations (1), (8), (14) | Equation (18) | Equation (20) | Equation (20) | [40] |
| <i>A. succiniciproducens</i> MBEL55E | Batch | Glucose | Combination of Equations (1), (8), (14) | Equation (19) | Equation (20) | Equation (20) | [83] |
| <i>Y. lipolytica</i> PCG0100 | Batch | Glycerol | Combination of Equations (1), (8), (14) | Equation (19) | Equation (20) | Equation (20) | [91] |

Lin et al., Pateraki et al., Song et al., Vlysidis et al. and Li et al. [38,40,83,86,91] have developed some of the most complete models of this type, predicting the evolution of the concentration of biomass, substrate, SA and by-products in reactions catalyzed by *A. succinogenes*, *B. succiniciproducens*, *M. succiniciproducens* and *Y. lipolytica*. Table 2 shows

a comparison of the parameters that describe the growth of biomass according to these authors. In all cases, a Monod model was used with inhibitions by a Haldane–Andrews type substrate and Luong type product, except in the case of the study carried out by Lin et al. [38], who have considered that an inhibition by substrate also follows a Luong model.

Table 2. Parameters from non-segregated unstructured biomass growth kinetic models.

| Microorganism | CarbonSource | Eqs. | Parameters | | | | | | Ref. | |
|---|--------------------------------|---------------|------------|------------|--|------------|------------|--|------|---------|
| | | | μ_m | $[S]_m$ | $[P]_m$ | K_S | K_{IS} | α | | β |
| | | | h^{-1} | $g L^{-1}$ | $g L^{-1}$ | $g L^{-1}$ | $g L^{-1}$ | | | |
| <i>A. succinogenes</i> ATCC 55618 | Glucose | (1) (11) (14) | 0.5 | 155 | SA-104.2 ET-42.1 AA-44.2 FA-16.0 PA-74.1 | 2.03 | | 0.603 | [38] | |
| <i>A. succinogenes</i> ATCC 55618 | Glycerol | (1) (8) (14) | 0.12 | | 45.6 | 2.896 | 15.36 | 1.074 | [86] | |
| <i>A. succinogenes</i> 130Z | Xylose galactose glucose | (1) (8) (14) | 0.394 | | AA-38 FA-18 LA-60 SA-55 | 0.698 | 55.484 | AA-2.300 FA-2.300 LA-/ SA-2.300 | [40] | |
| <i>B. succiniciproducens</i> JF 4016 | mannose arabinose | | 0.932 | | AA-38 FA-22 LA-58 SA-55 | 1.556 | 15.173 | AA-2.300 FA-2.299 LA-2.300 SA-2.299 | | |
| <i>M. succiniciproducens</i> MBEL55E | Glucose | (1) (8) (14) | 1.324 | | 17.23 | 1.123 | 88.35 | 1.301 | [83] | |
| <i>Y. lipolytica</i> PGC0100 | Glycerol | (1) (8) (14) | 0.38 | | AA-57.9 SA-243.4 | 0.818 | 223.5 | AA-12.02 SA-12.30 | [91] | |

As can be observed, the value of μ_m —Equations (5), (8), (11) and (14)—is between 0.12 and 1.324 h^{-1} depending on the microorganism and environmental factors. Some of the lowest values of this activity parameter are found in fermentations by *A. succinogenes*, being the lowest when glycerol was used as the substrate [86], followed by the one corresponding to the use of a mixture of sugars rich in xylose [40]. The maximum growth rate of *A. succinogenes* was reached using glucose as the carbon source [38], more than four times higher than when using glycerol [86]. Among the fermentations carried out with glucose as the carbon source, considerably higher μ_m values were achieved in the case where the biocatalyst was *M. succiniciproducens* [83] instead of *A. succinogenes* [38]. In the cases in which glycerol was used as a substrate, this parameter tripled when *Y. lipolytica* [91] was selected instead of *A. succinogenes* [86].

The values of the limiting nutrient concentration at which the specific growth rate is half of the maximum K_S —Equations (5), (8), (11)—are between 0.698 $g L^{-1}$ and 2.896 $g L^{-1}$. With *A. succinogenes*, Vlysidis et al. [86] achieved the highest value employing glycerol as the carbon source. The value estimated by Lin et al. [38] with the same microorganism turned out to be quite high as well (2.03 $g L^{-1}$) when glucose was used as a carbon source, but when opting for a carbon source rich in xylose, this value dropped drastically to 0.698 $g L^{-1}$, as observed by Pateraki et al. [40]. In fermentations with glucose, using *A. succinogenes*, the K_S was practically double [38] of that with *M. succinoproducens* [83]. In the operations with glycerol, the estimates made from the data obtained from the production carried out by *A. succinogenes* [86] were considerably higher (2.896 $g L^{-1}$) than when *Y. lipolytica* was used (0.818 $g L^{-1}$) [91]. Among the selected fermentations, an evaluation of the reported values of K_{IS} —Equations (8) and (11)—allows to conclude which are the strongest inhibitions due to the substrate. When working with *A. succinogenes*, a substrate mixture rich in xylose (55.48 $g L^{-1}$) turns out to be much less inhibitory [40] than glycerol (15.36 $g L^{-1}$) [86]. It

should be noted that, when glycerol is selected as the carbon source, inhibition falls when, instead of opting for this microorganism, *Y. lipolytica* yeast (223.5 g L⁻¹) is used [91].

According to the $[P]_m$ calculated by Lin et al. [38], the products that generated inhibition in the growth of *A. succinogenes* with glucose are SA, ethanol (ET), AA, FA and PA. Pateraki et al. [40], starting from a mixture of xylose and other sugars, observed inhibition by AA, FA, LA and SA. Vlysidis et al. [86] preferred to neglect the possible inhibitory effect of the by-products, including the assumption that only SA generates considerable inhibition in glycerol fermentation. Although Lin et al. [38] considered the inhibitory effect of various compounds using glucose as the carbon source, Song et al. [83] only included SA in their estimates in a process carried out with the same substrate but with *M. succiniproducens* as the biocatalyst. In the operations with glycerol, it seems that there are fewer species with inhibitory effects, with only SA being considered in both the studies by Vlysidis et al. [86] as in those of Li et al. [91], although the latter authors also considered the influence of FA.

Table 3 shows the parameters obtained by Lin et al., Pateraki et al., Vlysidis et al., Song et al. and Li et al. [38,40,83,86,91] in the study of the evolution of the concentrations of substrates and products in the fermentations. Lin et al. and Pateraki et al. [38,40] have proposed models in which the parameters of the kinetic models of substrate concentration are grouped into two constants. The first of them is δ (Equation (18)), which is associated with growth, thus encompassing the yields of biomass and product in a substrate). The other parameter is γ (Equation (18)), which is not associated with the growth of biomass but includes the yield of product in a substrate and the Pirt’s maintenance coefficient. On the other hand, Vlysidis et al., Song et al. and Li et al. [83,86,91] have considered that the yield of biomass in a substrate would be associated with the growth of biomass, whilst the yield of product in a substrate would be associated with the production of acid and the Pirt’s maintenance coefficient is multiplied by the biomass concentration (Equation (19)). Both δ (4.35–7.575 g g⁻¹) and γ (0.034–0.308 g g⁻¹ h⁻¹) are observed to reach the highest values in reactions catalyzed by *A. succinogenes*, especially when using a mixture of sugars rich in xylose [40]. Vlysidis et al., Song et al., Li et al. and [83,86,91] estimated that the evolution of the substrate could be studied considering exclusively the following parameters: the yield of this carbon source in biomass, the yield to SA in the substrate and the Pirt’s maintenance coefficient, the latter of which acquires a value practically of zero.

Table 3. Parameters from non-segregated unstructured kinetic models considering substrate consumption and product generation in SA production.

| Microorganism | Carbon Source | Substrate | | | | | Product and By-Products | | | Ref. | |
|---|--|-----------|-----------------|--|-------------------------------|-------|---|-----------------------------------|--|--|--|
| | | Eqs. | Parameters | | | Eqs. | Parameters | | | | |
| | | | Y _{XS} | Y _{Pis} | δ g g ⁻¹ | | γ g g ⁻¹ h ⁻¹ | m _s h ⁻¹ | α_i g g ⁻¹ | | β_i g g ⁻¹ h ⁻¹ |
| <i>A. succinogenes</i> ATCC 55618 | Glucose | (18) | | | 4.35 | 0.308 | | (20) | AA-1.430 FA-0.881 PA-0.187 SA-3.600 | AA-0.045 FA-0.013 PA-0.049 SA-0.299 | [38] |
| <i>A. succinogenes</i> ATCC 55618 | Glycerol | (19) | 0.130 | 2.790 | | | 0.001 | (20) | AA-0.753 FA-0.428 SA-9.864 | AA-0.001 FA-0.002 SA-0.001 | [86] |
| <i>A. succinogenes</i> 130Z | Xylose galactose glucose mannose arabinose | (18) | | | 7.575 | 0.051 | | (20) | AA-2.258 FA-1.882 LA-/ SA-3.858 | AA-2.136 FA-1.501 LA-0.419 SA-4.080 | [40] |
| <i>B. succiniciproducens</i> JF 4016 | | | | | 6.685 | 0.034 | AA-0.016 FA-0.006 LA-/ SA-0.040 | | AA-0.001 FA-0.001 LA-0.001 SA-0.028 | | |
| <i>M. succiniciproducens</i> MBEL55E | Glucose | (19) | 0.765 | AA-0.999 FA-1.532 LA-0.999 SA-1.310 | | | 0.061 | (20) | AA-0.626 FA-0.665 LA-/ SA-1.619 | AA-0.124 FA-0.105 LA-0.210 SA-0.355 | [83] |
| <i>Y. lipolytica</i> PGC0100 | Glycerol | (19) | 0.581 | AA-1.864 SA-1.712 | | | 0.055 | (20) | AA-0.208 SA-0.386 | AA-0.010 SA-0.013 | [91] |

It should be noted that, despite starting from glycerol in both cases, Vlysidis et al. [86] only considered the effect of SA carrying out the fermentation with *A. succinogenes*, while Li et al. [91] have also had to consider the inhibition generated by AA when using *Y. lipolytica* as a biocatalyst.

All the authors of these works consider that AA and SA produce an inhibitory effect on SA production—Equation (20)—[38,40,83,86,91]. Regarding the parameters associated with the growth of the microorganism, it can be observed that the effect of SA is the one with the highest values. For all microorganisms and substrates, the coefficient not associated with growth presents higher values for SA, except in the case of fermentation with *A. succinogenes* starting from glycerol [86], where the acid that generates the greatest impact in productivity is PA.

3. Mass Transfer Phenomena

In the previous section, we have compiled key information on the work of researchers that studied the evolution over time of the species involved in fermentation, proposing kinetic models and estimating parameters that allow for optimizing the system. However, to predict the distribution of the chemical species in the different phases in contact involved in a fermentation process, it is essential to conduct a preliminary analysis on the mass transfer among these phases. It is the joint knowledge and coupling of bio/chemical kinetics, heat and mass balances and transport phenomena that allows for carrying out an adequate design of the reactor and of the control system as well as the realization of a change and techno-economic studies, as explained above.

Microbial processes usually take place in triphasic systems (gas–liquid–solid), where the continuous phase is liquid, while the gas phase and the solid microorganisms can be considered as discontinuous phases in suspension or travelling through the liquid phase, usually aqueous. Nutrients and metabolites present a different resistance to transport depending on their molecular volume and the fluid dynamics of the phase or interface they are in. Nutrients' availability at the cellular level is key to achieving high yields. In addition, the gas–liquid transport of CO₂ in these systems acquires special relevance as CO₂ activates the SA generation route.

Until now, the studies carried out on the mass transfer of CO₂ are scarce and limited to very specific systems, and without application to cellular systems; therefore, it is important to highlight the importance of increasing knowledge in this area. Due to the multiple phenomena that take place at the same time, the mass transfer of CO₂ is difficult to estimate, being influenced by a large number of parameters, such as the physical properties of the gaseous and liquid phase, the operating conditions, the geometric parameters and the state of the biomass. In fermentations, biochemical processes and transport take place at the same time; therefore, it is essential to know the speed at which each one of them takes place and to know the limiting stages. For example, in the event that the rate of transport of the substrates to the cells is higher than the rate of metabolic reactions, the overall rate of conversion would depend on the kinetics of the biochemical reactions. In the opposite case, in which the transfer rate was lower than that of the reaction, it would be essential to make efforts to reduce the average time needed for mass transfer to prevent it from continuing to be the limiting stage. Thus, the study of the overall mechanism of their transfer can be outlined in several stages depending on the location, as shown in Figure 4 [92–95].

3.1. Mass Transport in the Liquid Phase

Due to the diffusivities of gases being relatively high compared to those of liquids (103–105 times higher), and their low solubility in water of common gases involved in bioprocesses, the transfer from the gas to the liquid phase is considered the limiting step of the overall process rate [96,97]. In particular, the study of CO₂ transfer is of great importance, since its presence is essential for the activation of the SA production pathway in the TCA cycle [29]. To deepen into this aspect, the following processes should be considered:

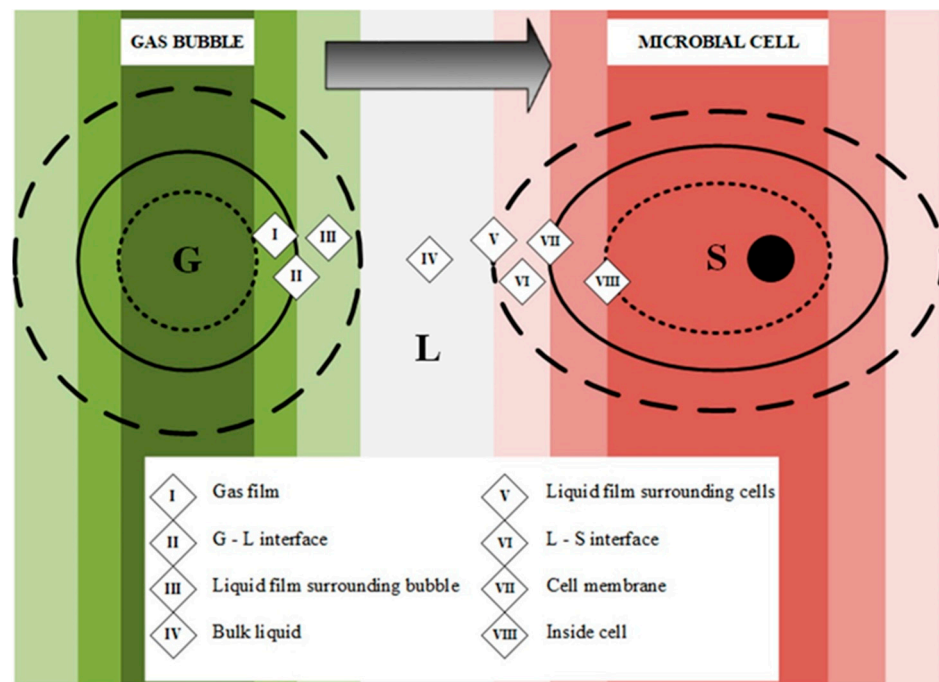


Figure 4. Steps involved in gas transfer from gas bubble to cell.

3.1.1.1. CO₂—Carbonate Equilibrium

When CO₂ dissolves in the fermentation broth, it undergoes a series of chemical equilibrium reactions that follows the model presented below, in which carbonic acid (H₂CO₃), bicarbonate ion (HCO₃⁻) and carbonate ion (CO₃²⁻) are involved [98–101].



The equilibrium constants for these three reactions (K₁, K₂, and K₃) can be expressed as follows:

$$K_1 = \frac{[H_2CO_3]}{[CO_2]} \tag{27}$$

$$K_2 = \frac{[HCO_3^-][H^+]}{[H_2CO_3]} \tag{28}$$

$$K_3 = \frac{[CO_3^{2-}][H^+]}{[HCO_3^-]} \tag{29}$$

Owing to the high instability of carbonic acid in solution and its tendency to dissociate and lose protons, Equations (24) and (25) combine to give Equation (30) [99,100], whose dissociation constant is shown in Equation (31):



$$K_4 = K_1 \times K_2 = \frac{[HCO_3^-][H^+]}{[CO_2]} \tag{31}$$

Furthermore, it must be taken into account that, in broths with a pH above 7 (and especially those above 8.5), a secondary reaction of hydroxylation of CO₂ with OH⁻ ions may predominate [102]: however, this equilibrium would not generally be predominant in

the production of succinic acid since, as mentioned above, the optimum operating pH is around 6.8.



Therefore, the total dissolved CO₂ (C_T) would be the sum of the concentration of CO₂, HCO₃⁻ and CO₃²⁻ as shown in Equation (33) [98,103,104]:

$$C_{TCO_2} = [CO_2] + [HCO_3^-] + [CO_3^{2-}] \tag{33}$$

Considering an approximately neutral pH, the proportion of CO₂ in the total carbonate (α) [98] would be:

$$\alpha = \frac{[CO_2]}{[CO_2] + [HCO_3^-] + [CO_3^{2-}]} \tag{34}$$

If the dissociation constants K₃ and K₄ (with values—at 39 °C—of K₃ = 6.12 10⁻¹¹ and K₄ = 5.35 10⁻⁷) are substituted in Equation (34), Equation (35) is obtained, which is a function of the concentration of dissolved protons [H⁺] [99,104,105]:

$$\alpha = \frac{1}{1 + \frac{K_4}{[H^+]} + \frac{K_3 \cdot K_4}{[H^+]^2}} \tag{35}$$

From Equations (33) and (35), Equation (36) is derived to obtain the CO₂ concentration [99,104–106]:

$$[CO_2] = \frac{C_T}{1 + \frac{K_4}{[H^+]} + \frac{K_3 \times K_4}{[H^+]^2}} \tag{36}$$

3.1.2. Gas–Liquid Equilibrium

From low to moderate pressures, Henry's law satisfies the ideal equilibrium condition between the liquid and gas phases; thus, Equation (37) can describe the solubility of CO₂ in a pure liquid [98,99,101,105–108]:

$$[CO_2] = \frac{P_{CO_2}}{H_0} \tag{37}$$

where [CO₂] is the concentration of dissolved CO₂ in a liquid (mol·L⁻¹), P_{CO₂} is the CO₂ partial pressure in a gas mixture (kPa) and H₀ is the Henry's constant for CO₂ in a pure solvent (kPa m³ kmol⁻¹).

Due to the fact that a culture medium contains salts and organic substances, it is necessary to describe the solubility of CO₂ using an empirical model such as that suggested by Schumpe and Deckwer—Equation (38). In this model, the salting-out effect of each ion on a given gas is assumed to be independent from the other ions present in the solution [105,106,108,109]:

$$\log\left(\frac{H}{H_0}\right) = \log\left(\frac{\alpha_0}{\alpha}\right) = \sum_i (h_i + h_G) \times C_i + \sum_j b_j \times C_{n,j} \tag{38}$$

where H is the Henry's constant in a media, α₀ and α are the Bunsen coefficients to express the CO₂ solubility within a wide temperature range, h is the ion coefficient, h_i (L·mol⁻¹) is the inorganic ion coefficient in the medium (Na⁺ = 0.1143; K⁺ = 0.0922; Ca²⁺ = 0.1762; Mg²⁺ = 0.1694; H⁺ = 0; Cl⁻ = 0.0318; HPO₄²⁻ = -0.1499; OH⁻ = 0.0839; HCO₃⁻ = 0.0967; CO₃²⁻ = 0.1423) [106], b_j and h_G are estimated by Equations (39) and (40), respectively, as suggested by Weisenberger and Schumpe [110], C_i is the concentration of ion i (mol·L⁻¹) and C_{n,j} is the concentration of organic substance j species (kg m⁻³).

$$h_G = h_{G,0} + h_{G,T}(T - 298.15) \tag{39}$$

$$b_j = b_n + b_G \tag{40}$$

Here, $h_{G,0}$ for CO₂ is 0.0172 L·mol⁻¹ and $h_{G,T}$ is 3.38·10⁻⁴ L mol⁻¹ K⁻¹ at temperatures between 273 and 313 K, T is the absolute temperature (K); b_n (m³ kg⁻¹) for yeast extract is 7.9 10⁻⁴, for glucose is 6.68 10⁻⁴ and for corn steep liquor is 2.11 10⁻⁴ [98]. b_G can be calculated using the Rischbieter Equation (41) [111]:

$$b_G = b_{G,0} + b_{G,T}(T - 298.15) \tag{41}$$

where $b_{G,0}$ for CO₂ is 1.86·10⁻⁴ m³ kg⁻¹ and $b_{G,T}$ is 0.01·10⁻⁴ m³ kg⁻¹ K⁻¹ at temperatures between 288 and 323 K [58,59,61].

From Henry’s constant H and the partial pressure of CO₂, C_T is obtained with Equation (42) [99,109]:

$$C_{T_{CO_2}} = \frac{[CO_2]}{\alpha_0} = \frac{P_{CO_2}}{\alpha_0 \times H} \tag{42}$$

3.1.3. Gas–Liquid Mass Transfer

The transfer of a component from one phase to another is determined by several complex processes including variables such as the interfacial contact area, concentration gradients, molecular diffusivities, mixing conditions, temperature and pressure as well as the rheological phenomena and chemical reactions. The volumetric mass transfer coefficient ($k_L a$) shows the effectiveness of this process considering these variables except for concentration gradients [92,101]; therefore, the carbon dioxide transfer rate (CTR) would be governed by Equation (43) [99,112,113]:

$$CTR = \frac{d[CO_2]}{dt} = k_L a \cdot ([CO_2^*] - [CO_2]) \tag{43}$$

where $[CO_2]$ is the concentration of dissolved CO₂ in the bulk liquid (mol L⁻¹), $[CO_2^*]$ is the saturated CO₂ concentration at a specific CO₂ partial pressure (mol L⁻¹), $k_L a$ is in units of reciprocal time and can be estimated with Equation (44) [114]:

$$k_L a = f \times \left(\frac{P_G}{V_w} \right)^a \times v_s^b \tag{44}$$

Here, f is a specific constant related to the geometry of the vessel, P_G/V_w is the gassed power requirement per working volume, V_s is the superficial gas velocity and constants a and b depend on the corresponding correlation.

As explained in the review by Elhajj et al. [101], due to the complexity of the hydrodynamic conditions, a large number of empirical mass transfer correlations have been developed for each system, which are only applicable under very specific conditions.

For well mixed reactors, Hill [115] proposed Equation (45) to calculate the CO₂ transfer, sparged from the bottom of the reactor, in the aqueous phase, not taking into account the bubble size:

$$CTR = \frac{d[CO_2]}{dt} = k_L a \times ([H_2CO_3^*] - [CO_2]) \left(1 - \frac{K_2}{K_2 + (K_2 \times [CO_2]^{0.5})} \right) \tag{45}$$

where $[H_2CO_3^*]$ is the saturation concentration of carbonic acid in aqueous solution and K_2 is the equilibrium constant of the aforementioned equilibrium reaction (25) of the deprotonation of carbonic acid to bicarbonate ion. $k_L a$ ranges from 5.6 to 33 10⁻³ s⁻¹ and is obtained by Equation (46):

$$k_L a = 33.9 + 6.96 \times \left(\frac{T - 27.5}{7.432} \right) + 15.7 \times \left(\frac{Q_G - 1.1}{0.5351} \right) + 18.8 \times \left(\frac{N - 375}{133.8} \right) \tag{46}$$

in which T is the temperature in °C, Q_G is the gas flow rate ($L \cdot \text{min}^{-1}$) and N is the stirring speed (rpm). This expression is valid under the following conditions: $15 \text{ }^\circ\text{C} < T < 40 \text{ }^\circ\text{C}$, $0.2 \text{ L min}^{-1} < Q_G < 2 \text{ L min}^{-1}$, and $150 \text{ rpm} < N < 600 \text{ rpm}$.

Because the method originally used for measuring CO_2 solubility and determining $k_L a$ was considered incorrect by Kordac and Linek, [101,116], they subsequently proposed Equation (47) as a new expression to estimate CTR . In this case, the following assumptions applies: the ideal mixing in the gas phase, negligible resistance to mass transfer in the gas phase, no consideration of the bubble size and the equilibrium reaction of CO_2 in the liquid phase being fast enough to keep carbonate, bicarbonate and hydrogen concentrations in equilibrium at all times.

$$CTR = \frac{d[\text{CO}_2]}{dt} = k_L a \cdot \left(\frac{A}{1 + A} \right) ([\text{H}_2\text{CO}_3^*] - [\text{CO}_2]) \left(\frac{2}{2 + \left(\frac{K_2}{[\text{CO}_2]} \right)^{0.5}} \right) \quad (47)$$

where A is calculated by Equation (48):

$$A = \frac{Q_G \cdot H}{k_L a \cdot V_w \cdot R \cdot T} \quad (48)$$

where Q_G is the gas flow in $L \text{ s}^{-1}$ while V_w is the volume of liquid in the reactor (L), R is the ideal gas constant ($\text{atm L mol}^{-1} \text{ K}^{-1}$) and T is the temperature in K. This correlation is applicable for the following conditions: $0.833 \cdot 10^{-4} \text{ m}^3 \cdot \text{s}^{-1} < Q_L < 1.5 \cdot 10^{-4} \text{ m}^3 \cdot \text{s}^{-1}$, $0.583 \cdot 10^{-3} \text{ m}^3 \text{ s}^{-1} < Q_G < 1.17 \cdot 10^{-3} \text{ m}^3 \text{ s}^{-1}$, and $0.05 < y_{\text{CO}_2} < 0.2$. K_L is a number between 2.06 and $4.69 \cdot 10^{-3} \text{ m s}^{-1}$.

Equation (49) is proposed to describe the response dynamics of the concentration of carbonic acid in the liquid. This expression can be simplified into Equation (50) assuming that the pH value remains lower than 5 during most of the CO_2 absorption experiments. With the relationship between B and A being established by Equation (51), $k_L a$ can finally be solved by Equation (52):

$$\frac{d[\text{H}_2\text{CO}_3]}{dt} = k_L a \times \frac{A}{1 + A} ([\text{H}_2\text{CO}_3^*] - [\text{H}_2\text{CO}_3]) \times \left(\frac{2}{2 + \left(\frac{K_2}{[\text{CO}_2]} \right)^{0.5}} \right) \quad (49)$$

$$\frac{d[\text{H}_2\text{CO}_3]}{dt} = k_L a \times \frac{A}{1 + A} 0.99 \times ([\text{H}_2\text{CO}_3^*] - [\text{H}_2\text{CO}_3]) = B \times ([\text{H}_2\text{CO}_3^*] - [\text{H}_2\text{CO}_3]) \quad (50)$$

$$B = k_L a \times \frac{A}{1 + A} \times 0.99 \quad (51)$$

$$k_L a = \left(\frac{0.99}{B} - \frac{V_L \times R \times T}{Q_G \times H} \right)^{-1} \quad (52)$$

3.2. Mass Transport and Biofilm

Low productivity in the biological production of succinic acid is one of the main obstacles to overcome in biorefineries [56,117]. For this, although most of the production studies are carried out in batch or fed-batch operated bioreactors, it is recommended to operate continuously and generate a biofilm, which allows cells to adhere to surfaces at high concentrations, achieving a steady state, non-growing condition and reaching much higher productivities and yields than with other systems [54–56,118]. Furthermore, operation under these conditions promotes the stability and tolerance to toxic substances and inhibitors, because these substances (substrates, products and toxic substances from the raw material hydrolysate, as furfurals or hydroxymethylfurfurals) do not accumulate in the bioreactor over time, diffusing into the biofilm in a restricted way—so their deleterious effect on cells are partly avoided—[119,120]; however, the study of transport phenomena

in biofilms poses a great challenge, since they do not have established and well-defined properties. Their structural and physical characteristics such as density, porosity, thickness, cohesion, and cell viability are largely determined by the conditions in which they have been created [119,120]. Unfortunately, all these characteristics and the difficulty to control many of them makes the study of these structures very complex, which has led mostly to the development of equations of a strong empirical character. Biofilm structures are highly irregular with cells showing a tendency to aggregate, thus forming cellular microcolonies of a varying area, shape, and thickness. These microcolonies usually have smaller areas near the surface of the substrate, while the area increases towards the top of the biofilm. This sometimes leads to their fusion, generating even larger microcolonies [121]; therefore, it is logical that the average effective diffusivity (D_e) is dependent on the density, as expressed by Equation (53) [122], and varies along the biofilm—Equations (54) and (55) [123]:

$$D_e = D \left(1 - \frac{0.43 \times \rho_b^{0.92}}{11.19 + 0.27 \times \rho_b^{0.99}} \right) \tag{53}$$

$$D_e = \sum_{n=1}^p D_{S,n} \tag{54}$$

$$D_s = 0.25 - 0.95 \times v_L + 2.3 \times [G] + 0.23 \times \left(\frac{z}{L_j} \right) + 0.93 \times v_L \times [G] + 0.59 \times v_L \times \left(\frac{z}{L_b} \right) - 0.7 \times [G] \times \left(\frac{z}{L_b} \right) \tag{55}$$

where ρ_b is the average density of the biofilm ($\text{kg}\cdot\text{m}^{-3}$), D is the molecular diffusivity of the reactive species in the medium ($\text{m}^2\cdot\text{s}^{-1}$), D_s is the surface averaged relative effective diffusivity, p is the number of measurement points of surface average relative effective diffusivity (vertically), v_L is the velocity in the bulk liquid ($\text{m}\cdot\text{s}^{-1}$), $[G]$ is the glucose concentration ($\text{kg}\cdot\text{m}^{-3}$), z is the distance from the bottom of the biofilm (m) and L_b is the average biofilm thickness.

Mokwatlo et al. [124], using Equations (56)–(58), estimated the constant D_{e-j} , which means the effective diffusion constant of compound j in the biofilm as related to the aqueous diffusion constant:

$$\frac{D_{eo-j}}{D_{aq-j}} = \varepsilon_W \times \left(\frac{\varepsilon_{EPS}}{D_{pr}} + \varepsilon_W \right)^{-1} \tag{56}$$

$$\frac{D_{e-j}}{D_{aq-j}} = \left(\frac{D_{e-j}}{D_{eo-j}} \right) \times \left(\frac{D_{eo-j}}{D_{aq-j}} \right) \tag{57}$$

$$\frac{D_{e-j}}{D_{eo-j}} = \left(\frac{\frac{2}{D_{cr}} + \frac{D_{aq-j}}{D_{eo-j}} - 2 \times \varepsilon_{cells} \cdot \left(\frac{1}{D_{cr}} - \frac{D_{aq-j}}{D_{eo-j}} \right)}{\frac{2}{D_{cr}} + \frac{D_{aq-j}}{D_{eo-j}} + \varepsilon_{cells} \times \left(\frac{1}{D_{cr}} - \frac{D_{aq-j}}{D_{eo-j}} \right)} \right) \tag{58}$$

where D_{aq-j} is the diffusion constant of j in water ($\text{m}^2\cdot\text{s}^{-1}$), D_{eo-j} the effective diffusion constant of j in “cell free” extracellular polymeric substances/water matrix ($\text{m}^2\cdot\text{s}^{-1}$), ε_{cells} the biofilm volume fractions of the cells, ε_{EPS} the biofilm volume fractions of extracellular polymeric substances y , and ε_W the biofilm volume fractions of water.

To relate convective mass transfer and mass diffusivity, Horn and Hempel proposed an empirical Equation (59) to calculate the Sherwood number (Sh) [125]:

$$Sh = 2 \times Re^{0.5} \times Sc^{0.5} \times \left(\frac{d}{L} \right)^{0.5} \cdot (1 + 0.0021 \times Re) \tag{59}$$

where Re is the Reynolds number, Sc is the Schmidt number, d is the diameter of the reactor and L is the length of the reactor.

Wäsche et al. [126] accounted for the influence of the biofilm structure on mass transfer, for which they introduced a structure factor (Ω) in the expression of the Sherwood number.

Furthermore, they distinguished expressions for the calculation of this number in the laminar regime—Equation (60)—and the turbulent regime—Equation (61).

$$Sh_{laminar} = 2 \times Re^{0.5} \times Sc^{0.5} \times \left(\frac{d}{L}\right)^{0.5} \times \Omega^{-1} \tag{60}$$

$$Sh_{turbulent} = 0.16 \times Re^{0.75} \times Sc^{0.5} \times \Omega^{-1} \tag{61}$$

The structure factor depends on the hydrodynamic and substrate conditions during the biofilm culture, as shown in Equation (62), and it is a function of the Reynolds number as defined in Equation (63):

$$\Omega = 6^{6 \times \mu^*} \times Re_{growth}^{-\left(\frac{\mu^*}{15}\right)} \tag{62}$$

$$Re_{growth} = \frac{w \times d}{\nu} \tag{63}$$

where μ^* is the relative growth rate, i.e., the ratio between the specific growth rate at the biofilm surface and the maximum growth rate, w is the mean flow velocity ($m \cdot s^{-1}$) and ν is the kinematic viscosity of water ($m^2 \cdot s^{-1}$).

4. Coupling Dynamic Phenomena to Explain Succinic Acid Production

As challenging as it may be, a comprehensive study of the behavior of the species present in a fermentation broth must jointly consider reaction kinetics and transport phenomena; however, the complexity of these models has meant that their analysis and development is limited and only a couple of studies have appeared in this regard. The combination of dynamic phenomena and kinetic models allows complete information on the system to be obtained, as mentioned above, being a fundamental tool when optimally designing the reactor, scaling-up, carrying out technical-economic studies and developing a system of control. In addition, knowledge about the optimal flow of CO₂ and the way to achieve an adequate transfer, allows to reduce the costs associated with the feeding of this gas (for example, insufflation expenses, agitation and the capture of excess gas); therefore, in order to achieve the biological production of succinic acid in a sustainable manner, combining the techno-economic and environmental perspectives, the development of knowledge in this area is essential.

Galaction et al. [127] proposed equations to estimate the concentration and flux of glucose as a substrate in a stirred bed of immobilized *A. succinogenes* cells on alginate. For this purpose, they proposed a kinetic model in the mass balance of glucose in the biocatalyst including inhibition by a substrate and product of the Jerusalimsky type. As further assumptions to the model, they assumed steady state, spherical biocatalyst particles, no interactions between the substrate, product and support, and internal diffusion described according to Fick's law and effective diffusivity. From these constraints, Equation (64) is derived, from which Equations (67) and (68) are obtained, taking into account the boundary conditions—Equations (65) and (66):

$$\frac{d[P]}{dt} = \frac{D \times [P]}{[X]} \tag{64}$$

$$\frac{d^2[S]_P}{dr^2} + \frac{2}{r} \times \frac{d[S]_P}{dr} = \frac{v_{max} \times [X]}{D_e} \times \left(\frac{K_{IS}}{K_{IS} + [S]_P}\right) \times \left(\frac{K_{IP}}{K_{IP} + Y_{P/S} \times [S]_P}\right) \tag{65}$$

$$\text{s.t. : } r = 0 \rightarrow \frac{d[S]_P}{dr} = 0 \tag{66}$$

$$\text{s.t. : } r = R_P \rightarrow -D_e \cdot \frac{d[S]_P}{dr} = k_L \times ([S]_L - [S]_S) \tag{67}$$

$$[S]_P = \frac{Bi \times ([S]_L - [S]_s) \times \cosh(3 \times \varphi \times R_P)}{R_P^2} \times \left[\frac{3 \times \varphi}{R_P} - R_P \times \tanh(3 \times \varphi \times R_P) \right] \times \frac{\sinh(3 \times \varphi \times r)}{r} \quad (68)$$

where r is the radius of the particle, $[S]_P$ is the concentration of substrate within the biocatalyst particle, v_{max} is the maximum reaction rate, $[X]$ is the cell concentration, $[S]_L$ is the concentration in the liquid bulk, $[S]_s$ is the concentration on the surface of the biocatalyst particle, Bi is the Biot number, φ is the Thiele modulus and k_L represents the mass transfer coefficient in the boundary layer at the particle surface.

The substrate flux from the liquid phase to the particle surface (n_L) is described by Equation (69) and the internal mass flow (n_P) can be obtained by combining Fick's law with Equation (67), thereby obtaining Equation (70):

$$n_L = k_L \times ([S]_L - [S]_i) \quad (69)$$

$$n_P = D_e \frac{Bi \times ([S]_L - [S]_i) \times \cosh(3 \times \varphi \times R_P)}{R_P^2} \times [3 \times \varphi - R_P \times \tanh(3 \times \varphi \times R_P)] \times \left[\frac{3 \times \varphi \times \cosh\left(\frac{3 \times \varphi \times r}{R_P}\right) \sinh(3 \times \varphi \times r)}{R_P \times r} \right] \quad (70)$$

From these expressions, it was estimated that the inhibition is more pronounced in the smallest particles, whilst in the larger particles, internal diffusion is the main limiting step. In fact, in some internal regions of the particle it is possible to reach such low values of the flux that they are considered "biologically inactive regions", with a magnitude varying from 0 to 5.53% of the total volume of particles.

Later, the same authors [128] expanded this study, performing fermentation in a bioreactor with a stationary basket bed of immobilized *A. succinogenes* cells on alginate. In their study, they found that the values of the external mass flows were about 1.4 to 14 times lower than those obtained for the mobile bed, the difference being more important as the biocatalyst particle size increased and the cylindrical-bed thickness decreased. In this case, the biologically inactive region could be even higher, with its magnitude varying between 0.24% and 44% from the overall volume of each biocatalyst particle size studied and being found mostly in the largest particles on the outer surface of the bed of the basket. In addition to the equations used in their previous article, they included the reduction factor (λ). With a similar nature to the classical effectiveness factor (η), λ represents the ratio between the rates of biochemical reaction in heterogeneous and homogeneous systems. Considering Equation (64), the reduction factor can be expressed by Equation (71):

$$\lambda = \frac{3 \times k_L \times ([S]_L - [S]_i) \times \cosh(3 \times \varphi \times R_P)}{R_P^4 \times v_{max} \times [C]} \times \frac{\left[\frac{3 \times \varphi}{R_P} - R_P \times \tanh(3 \times \varphi \times R_P) \right] \times \cosh(3 \times \varphi) \times [3 \times \varphi - \tanh(3 \times \varphi)]}{\left(\frac{K_{JS}}{K_{JS} + [S]_P} \right) \times \left(\frac{K_{JP}}{K_{JP} + Y_{P/S} \times [S]_P} \right)} \quad (71)$$

Although these balances include glucose transport as a substrate and reaction kinetics, they fail to include CO₂ transport, an essential molecule for the activation of the metabolic pathway for the production of SA. Rigaki et al. [114] proposed a mechanistic double substrate model to describe the fermentation by *A. succinogenes* of glycerol in batch systems saturated with CO₂. With this model, it is possible to predict the effect of changes in the initial concentrations of glycerol and MgCO₃ on the production and consumption rates of the species present in the broth. The evolution of biomass correlates with Equation (72), which is based on the Monod model—Equation (4)—a Luong-type product inhibition—Equation (14)—and also includes a transport term that includes the mass transfer coefficient (k_L):

$$\frac{d[X]}{dt} = \mu_m \times \left(\frac{[Gly]}{K_{Gly} + [Gly]} \right) \times \left(\frac{[CO_2]}{K_{CO_2} + [CO_2]} \right) \times \left(1 - \frac{[P]}{[P]_m} \right)^\beta - k_L \times [X] \quad (72)$$

The concentrations of the products evolve according to Equation (20) and the concentrations of the substrates (glycerol and CO₂) are predicted by means of Equation (19), but in the case of CO₂, the CTR—Equation (43)—is added to this expression, obtaining Equation (73). Considering turbulent mixing and a low viscosity fermentation medium, $k_L a$ fits the empirical expression (74). The expressions of the terms involved in this equation are shown in Equations (75) and (76):

$$\frac{d[\text{CO}_2]}{dt} = \left(-\frac{1}{Y_{X[\text{CO}_2]}} \right) \frac{d[X]}{dt} + \left(-\sum_i \frac{1}{Y_{P_i[\text{CO}_2]}} \right) \frac{dP_i}{dt} + (-m)[X] + k_L a \times ([\text{CO}_2^*] - [\text{CO}_2]) \quad (73)$$

$$k_L a = (2.0 + 2.8 \cdot N) \times \left(\frac{P_g}{V_w} \right)^{0.77} \times v_s^{0.67} \quad (74)$$

$$P_G = q \cdot \left(\frac{P_o^2 \times N \times d^3}{Q^{0.56}} \right)^{0.45} \quad (75)$$

$$P_o = 0.035 \times \mu \times N^3 \times d^{3.7} \times W \times B^{0.8} \times R^{0.4} \times J^{0.3} \quad (76)$$

where P_g is the gas power requirement, V_w the working volume, v_s the superficial gas velocity, q is the impeller type, d the reactor diameter, Q the volumetric flow rate, P_o the power requirement for non-gassed Newtonian fluids, B the number of blades, W their width, R the number of baffles, J their width and μ the dynamic viscosity of the medium.

5. Conclusions

Succinic acid has emerged as a very interesting biobased product that could play a pivotal role in the future of biorefineries due to its applications and representing a building block to a wide array of products. This piece of work has summarized and presented systematically the available information on the kinetic modelling of fermentations to this valuable product in the open literature.

The study of a process focused on its implementation at an industrial level, and, therefore, of a bioprocess, requires an approach from the perspective of chemical engineering. In this review, the existing information on the succinic acid production process by biotechnological means has been gathered, focusing on the mathematical models used by different authors for the description of all the physical and chemical (or biochemical) phenomena involved in the overall rate of the process. The scarcity of global models capable of simulating the complex behavior of the system is highlighted.

There have been good attempts at describing fermentations with microorganisms that are known to perform them. In addition, overall, the models developed are also scarce from the point of view of the still relatively low variety of substrates employed in the studies. In general, the proposed kinetic models are very restricted, being mostly non-segregated and unstructured without considering in any case the effects of hydrodynamic stress. Moreover, due to the complexity not only of the chemical reaction network but also the set of mass transports involved, the great challenge of combining transport phenomena with a kinetic model in the bioprocess still remains largely unsolved.

The publications are scarce and provide partial information, focusing on the resistance of the solid substrate through the biofilm or on the transport of CO₂. Whilst all of this in principle represents a complication towards an accurate numerical description and prediction of the process, it also opens an opportunity for researchers in the field and the development of experimental and numerical methodologies. The development of kinetic models and their coupling to equations describing transport phenomena are essential to take into account, together with the mass and heat balances relevant to the bioreactor of interest, when it comes to a detailed design control and operation of the bioreactor, as the most critical unit within any bioprocess. This is key to reducing the operating costs through techno-economical optimization and guides the scaling-up of prototypes and control systems.

Author Contributions: Conceptualization, I.A.E., M.W. and M.L.; methodology, I.A.E., M.W. and M.L.; investigation, I.A.E.; writing—original draft preparation, I.A.E.; writing—review and editing, I.A.E., M.W., J.E., M.L. and V.E.S.; supervision, M.W., J.E., M.L. and V.E.S.; project administration, M.L. and V.E.S.; funding acquisition, M.L. All authors have read and agreed to the published version of the manuscript.

Funding: This work was kindly supported by the Spanish Science and Innovation Ministry through three research projects: CTQ-2013-45970-C2-1-R, CTQ2017-84963-C2-1-R and PID2020-114365RB-C21, funding that is gratefully acknowledged.

Data Availability Statement: Not applicable.

Conflicts of Interest: The authors declare no conflict of interest.

Abbreviations

| | |
|--------------------|---|
| AA | Acetic Acid |
| ADP | Adenosine DiPhosphate |
| ATP | Adenosine TriPhosphate |
| CTR | Carbon dioxide Transfer Rate |
| C4 | 4 Carbon containing compound |
| C5 | 5 Carbon containing compound |
| C6 | 6 Carbon containing compound |
| ET | Ethanol |
| FAD+ | Flavin Adenine Dinucleotide |
| FA | Formic Acid |
| Fructose 1, 6-P | Fructose 1, 6-Phosphate |
| Fructose 6-P | Fructose 6-Phosphate |
| GDP | Gross Domestic Product |
| Glucose 6-P | Glucose 6 Phosphate |
| Glyceraldehyde 3-P | Glyceraldehyde 3-Phosphate |
| IB | Integrated Biorefineries |
| LA | Lactic Acid |
| NADH | Nicotinamide Adenine Dinucleotide reduced |
| NAD+ | Nicotinamide Adenine Dinucleotide |
| PA | Pyruvic Acid |
| PEP | Phosphoenol Pyruvate |
| PEPC | Phosphoenol Pyruvate Carboxylase |
| PEPCK | Phosphoenol Pyruvate Carboxykinase |
| PYC | Pyruvate Carboxylase |
| TCA | TriCarboxylic Acid Cycle |
| TRL | Technology Readiness Level |
| Ribose 5-P | Ribose 5-Phosphate |
| Ribulose 5-P | Ribulose 5-Phosphate |
| ROS | Reactive Oxygen Species |
| R+D+I | Research, Development and Innovation |
| SA | Succinic Acid |
| Sedoheptulose 7-P | Sedoheptulose 7-Phosphate |
| US DOE | United States Department of Energy |
| Xylulose 5-P | Xylulose 5-Phosphate |
| a | volumetric coefficient (m^3), exponent in Equation (21). |
| b | Schenov constant of organic substances ($\text{m}^3 \cdot \text{kg}^{-1}$), exponent in Equation (21) |
| B | number of blades |
| Bi | Biot number |
| C | concentration ($\text{mol} \cdot \text{L}^{-1}$, kg L^{-1}) |
| d | diameter of the reactor (m) |
| D | diffusivity ($\text{m}^2 \text{ s}^{-1}$), dilution rate (g L^{-1}) |
| D_e | effective diffusivity ($\text{m}^2 \text{ s}^{-1}$) |
| E | Euler number |

| | |
|---------------------------|--|
| f | specific constant related to the geometry of the vessel |
| h | Schenov constant of salts (L mol^{-1}) |
| H_0 | Henry's constant for CO_2 in a pure solvent ($\text{kPa m}^3 \text{ kmol}^{-1}$) |
| J | width of baffles (m) |
| k | mass transfer coefficient (m s^{-1}) |
| K | equilibrium constants, kinetic constants (g L^{-1}) |
| L | biofilm thickness, length of the reactor (m) |
| m | Pirt's coefficient (s^{-1}) |
| n | number of species, substrate flux ($\text{g m L}^{-1} \text{ s}^{-1}$), exponent of Equation (42) |
| N | stirring speed (rpm) |
| p | number of measurement points of surface average relative effective diffusivity |
| P | partial pressure in a gas mixture (kPa), power input under gassed conditions (W) |
| q | impeller type |
| Q | flow (L s^{-1} , L min^{-1}) |
| r | particle radius (m) |
| R | ideal gas constant ($\text{atm L mol}^{-1} \text{ K}^{-1}$), rate of metabolite production ($\text{g L}^{-1} \text{ h}^{-1}$), number of baffles |
| Re | Reynolds number |
| Sc | Schmidt number |
| Sh | Sherwood number |
| t | time (s, min, h) |
| T | temperature ($^{\circ}\text{C}$, K) |
| v | gas velocity, velocity in the bulk liquid (m s^{-1}) |
| V | volume of the liquid (L, m^3) |
| w | average flow velocity (m s^{-1}) |
| W | width of blades (m) |
| Y | yield (g g^{-1}) |
| Z | distance from the bottom of the biofilm (m) |
| $[\text{CO}_2]$ | concentration of dissolved CO_2 in the bulk liquid (mol L^{-1}) |
| $[\text{CO}_3^{2-}]$ | concentration of carbonate ion (mol L^{-1}) |
| [G] | glucose concentration (kg m^{-3}) |
| $[\text{H}_2\text{CO}_3]$ | carbonic acid concentration (mol L^{-1}) |
| $[\text{HCO}_3^-]$ | bicarbonate ion concentration (mol L^{-1}) |
| [P] | product concentration (g L^{-1}) |
| [S] | substrate concentration (g L^{-1}) |
| [X] | biomass concentration (g L^{-1}) |
| α | solubility of CO_2 , associated growth parameter in production generation models (g g^{-1}), exponent in Equation (48). |
| β | non-associated growth parameter in production generation models ($\text{g g}^{-1} \text{ h}^{-1}$), exponent of Equation (51). |
| δ | associated growth parameter in substrate consumption models (g g^{-1}) |
| γ | associated growth parameter in substrate consumption models ($\text{g g}^{-1} \text{ h}^{-1}$) |
| η | effectiveness factor |
| φ | Thiele modulus |
| λ | time of the latency phase (h), reduction factor |
| μ | specific growth rate (s^{-1} , min^{-1} , h^{-1}), dynamic viscosity ($\text{kg m}^{-1} \text{ s}^{-1}$) |
| ν | reaction rate ($\text{kg kg}^{-1} \text{ s}^{-1}$), kinematic viscosity ($\text{m}^2 \text{ s}^{-1}$) |
| ρ | density (kg m^{-3}) |
| Ω | structure factor |
| aq | refers to aqueous |
| b | refers to biofilm |
| cells | refers to cells in biofilm |
| EPS | refers to extracellular polymeric substances |
| G | refers to gas |
| i | refers to ion I, to species i |
| IS | refers to inhibition per substrate |

| | |
|------------------|--|
| j | refers to species j |
| L | refers to bulk liquid |
| m | refers to maximum state |
| n | refers to organic substances |
| o | refers to non-gassed Newtonian fluids, refers to “cell free” extracellular polymeric substances/water matrix |
| P | refers to product, biocatalyst particle |
| s | refers to superficial gas, refers to the surface of the biofilm, refers to the surface of the biocatalyst particle |
| S | refers to substrate |
| TCO ₂ | refers to total CO ₂ |
| T | refers to a specific temperature |
| w | refers to working volume, refers to water in biofilm |
| 0 | refers to a pure solvent or ambient conditions |
| 1 | refers to Equation (1) |
| 2 | refers to Equation (2) |
| 3 | refers to Equation (3) |
| 4 | refers to Equation (4) |
| * | refers to a relative rate, refers to a saturation concentration |

References

1. The World Bank Data GDP (Constant 2010 USD). Available online: <https://data.worldbank.org/indicator/NY.GDP.MKTP.KD> (accessed on 4 January 2022).
2. Parry, I.; Black, S.; Vernon, N.; Blewer, P.; Fulwood, M.; Khanburg, T.; Peciccia, A.; Roaf, J.; Schulz, P.; Zhunussova, K. *Still Not Getting Energy Prices Right: A Global and Country Update of Fossil Fuel Subsidies*; Elsevier: Amsterdam, The Netherlands, 2021.
3. Bechthold, I.; Bretz, K.; Kabasci, S.; Kopitzky, R.; Springer, A. Succinic Acid: A New Platform Chemical for Biobased Polymers from Renewable Resources. *Chem. Eng. Technol. Ind. Chem. Plant Equip. Process Eng. Biotechnol.* **2008**, *31*, 647–654. [[CrossRef](#)]
4. Martins, F.; Felgueiras, C.; Smitkova, M.; Caetano, N. Analysis of Fossil Fuel Energy Consumption and Environmental Impacts in European Countries. *Energies* **2019**, *12*, 964. [[CrossRef](#)]
5. Farrow, A.; Miller, K.A. *Toxic Air: The Price of Fossil Fuels*; Greenpeace: Amsterdam, The Netherlands, 2020.
6. Kotcher, J.; Maibach, E.; Choi, W.T. Fossil Fuels Are Harming Our Brains: Identifying Key Messages about the Health Effects of Air Pollution from Fossil Fuels. *BMC Public Health* **2019**, *19*, 1–12. [[CrossRef](#)] [[PubMed](#)]
7. Lelieveld, J.; Klingmüller, K.; Pozzer, A.; Burnett, R.T.; Haines, A.; Ramanathan, V. Effects of Fossil Fuel and Total Anthropogenic Emission Removal on Public Health and Climate. *Proc. Natl. Acad. Sci. USA* **2019**, *116*, 7192–7197. [[CrossRef](#)]
8. Kopel, J.; Brower, G.L. Impact of Fossil Fuel Emissions and Particulate Matter on Pulmonary Health. *Bayl. Univ. Med. Cent. Proc.* **2019**, *32*, 636–638. [[CrossRef](#)]
9. FitzPatrick, M.; Champagne, P.; Cunningham, M.F.; Whitney, R.A. A Biorefinery Processing Perspective: Treatment of Lignocellulosic Materials for the Production of Value-Added Products. *Bioresour. Technol.* **2010**, *101*, 8915–8922. [[CrossRef](#)]
10. Lipnizki, F.; Rudolph, G.; Thuvander, J. Membrane Processes in Lignocellulosic Biorefineries: Status, Potential and Challenges; Conference of Visegrad Countries. 2019. Available online: <https://lup.lub.lu.se/record/55f7df81-6d21-41b7-ae47-31de95c3c88b> (accessed on 7 January 2022).
11. Hassan, S.S.; Williams, G.A.; Jaiswal, A.K. Lignocellulosic Biorefineries in Europe: Current State and Prospects. *Trends Biotechnol.* **2019**, *37*, 231–234. [[CrossRef](#)]
12. Ubando, A.T.; Felix, C.B.; Chen, W.H. Biorefineries in Circular Bioeconomy: A Comprehensive Review. *Bioresour. Technol.* **2020**, *299*, 122585. [[CrossRef](#)]
13. Ali, N.; Zhang, Q.; Liu, Z.Y.; Li, F.L.; Lu, M.; Fang, X.C. Emerging Technologies for the Pretreatment of Lignocellulosic Materials for Bio-Based Products. *Appl. Microbiol. Biotechnol.* **2020**, *104*, 455–473. [[CrossRef](#)]
14. Usmani, Z.; Sharma, M.; Awasthi, A.K.; Lukk, T.; Tuohy, M.G.; Gong, L.; Nguyen-Tri, P.; Goddard, A.D.; Bill, R.M.; Nayak, S.C.; et al. Lignocellulosic Biorefineries: The Current State of Challenges and Strategies for Efficient Commercialization. *Renew. Sustain. Energy Rev.* **2021**, *148*, 111258. [[CrossRef](#)]
15. Yousuf, A.; Pirozzi, D.; Sannino, F. *Fundamentals of Lignocellulosic Materials for Bio-Based Products*; Academic Press: Cambridge, MA, USA, 2020.
16. Zuccaro, G.; Pirozzi, D.; Yousuf, A. Lignocellulosic Biomass to Biodiesel. In *Lignocellulosic Biomass to Liquid Biofuels*; Academic Press: Cambridge, MA, USA, 2020; pp. 127–167.
17. Ma, S.; Wang, H.; Li, J.; Fu, Y.; Zhu, W. Methane Production Performances of Different Compositions in Lignocellulosic Biomass through Anaerobic Digestion. *Energy* **2019**, *189*, 116190. [[CrossRef](#)]

18. Koupaie, E.H.; Dahadha, S.; Lakeh, A.B.; Azizi, A.; Elbeshbishy, E. Enzymatic Pretreatment of Lignocellulosic Biomass for Enhanced Biomethane Production—A Review. *J. Environ. Manag.* **2019**, *233*, 774–784. [CrossRef]
19. Salvachúa, D.; Mohagheghi, A.; Smith, H.; Bradfield, M.F.A.; Nicol, W.; Black, B.A.; Bidy, M.J.; Dowe, N.; Beckham, G.T. Succinic Acid Production on Xylose-Enriched Biorefinery Streams by *Actinobacillus succinogenes* in Batch Fermentation. *Biotechnol. Biofuels* **2016**, *9*, 28. [CrossRef]
20. Hassan, S.S.; Williams, G.A.; Jaiswal, A.K. Moving towards the Second Generation of Lignocellulosic Biorefineries in the EU: Drivers, Challenges and Opportunities. *Renew. Sustain. Energy Rev.* **2019**, *101*, 590–599. [CrossRef]
21. Pateraki, C.; Patsalou, M.; Vlysidis, A.; Kopsahelis, N.; Webb, C.; Koutinas, A.A.; Koutinas, M. *Actinobacillus succinogenes*: Advances on Succinic Acid Production and Prospects for Development of Integrated Biorefineries. *Biochem. Eng. J.* **2016**, *112*, 285–303. [CrossRef]
22. Sahoo, K.K.; Datta, S.; Nayak, A.; Pranaw, K.; Dutta, D.; Goswami, G. Biological Production of Succinic Acid: State of the Art and Future Perspectives. In *Industrial Microbiology and Biotechnology*; Springer: Singapore, 2022; pp. 427–461.
23. Bozell, J.J.; Petersen, G.R. Technology Development for the Production of Biobased Products from Biorefinery Carbohydrates—The US Department of Energy’s “Top 10” Revisited. *Green Chem.* **2010**, *12*, 539–554. [CrossRef]
24. Werpy, T.; Petersen, G. *Top Value Added Chemicals from Biomass: Volume I—Results of Screening for Potential Candidates from Sugars and Synthesis Gas (No. DOE/GO-102004-1992)*; National Renewable Energy Lab: Golden, CO, USA, 2004.
25. Putri, D.N.; Sahlan, M.; Montastruc, L.; Meyer, M.; Negny, S.; Hermansyah, H. Progress of Fermentation Methods for Bio-Succinic Acid Production Using Agro-Industrial Waste by *Actinobacillus succinogenes*. *Energy Rep.* **2020**, *6*, 234–239. [CrossRef]
26. McKinlay, J.B.; Vieille, C.; Zeikus, J.G. Prospects for a Bio-Based Succinate Industry. *Appl. Microbiol. Biotechnol.* **2007**, *76*, 727–740. [CrossRef]
27. Song, H.; Lee, S.Y. Production of Succinic Acid by Bacterial Fermentation. *Enzym. Microb. Technol.* **2006**, *39*, 352–361. [CrossRef]
28. Zeikus, J.G.; Jain, M.K.; Elankovan, P. Biotechnology of Succinic Acid Production and Markets for Derived Industrial Products. *Appl. Microbiol. Biotechnol.* **1999**, *51*, 545–552. [CrossRef]
29. Mancini, E.; Mansouri, S.S.; Gernaey, K.V.; Luo, J.; Pinelo, M. From Second Generation Feed-Stocks to Innovative Fermentation and Downstream Techniques for Succinic Acid Production. *Crit. Rev. Environ. Sci. Technol.* **2019**, *50*, 1–45. [CrossRef]
30. Akhtar, J.; Idris, A.; Aziz, R.A. Recent Advances in Production of Succinic Acid from Lignocellulosic Biomass. *Appl. Microbiol. Biotechnol.* **2014**, *98*, 987–1000. [CrossRef] [PubMed]
31. Polly, O.L. Production of Succinic Acid. U.S. Patent No. 2,533,620, 12 December 1950. Available online: <https://patents.google.com/patent/US2533620A/en> (accessed on 10 January 2022).
32. Cok, B.; Tsiropoulos, I.; Roes, A.L.; Patel, M.K. Succinic Acid Production Derived from Carbohydrates: An Energy and Greenhouse Gas Assessment of a Platform Chemical toward a Bio-Based Economy. *Bioprod. Biorefining* **2014**, *8*, 16–29. [CrossRef]
33. Dai, Z.; Guo, F.; Zhang, S.; Zhang, W.; Yang, Q.; Dong, W.; Jiang, M.; Ma, J.; Xin, F. Bio-based Succinic Acid: An Overview of Strain Development, Substrate Utilization, and Downstream Purification. *Biofuels Bioprod. Biorefining* **2019**, *14*, 965–985. [CrossRef]
34. Dienst, S.; Onderzoek, L. *Strategic Thinking in Sustainable Energy from the Sugar Platform to Biofuels and Biochemicals Final Report for the European Commission Directorate—General Energy*; Consorzio per La Ricerca e La Dimostrazione Sulle Energie Rinnovabili (RE-CORD): Florence, Italy, 2015.
35. MRP Global Bio Succinic Acid Market Insights, Forecast to 2026. Available online: <https://www.marketresearchplace.com/report/global-bio-succinic-acid-market-insights-forecast-to-192517.html> (accessed on 11 January 2022).
36. Mancini, E.; Dickson, R.; Fabbri, S.; Udagama, I.A.; Ullah, H.I.; Vishwanath, S.; Gernaey, K.V.; Luo, J.; Pinelo, M.; Mansouri, S.S. Economic and Environmental Analysis of Bio-Succinic Acid Production: From Established Processes to a New Continuous Fermentation Approach with in-Situ Electrolytic Extraction. *Chem. Eng. Res. Des.* **2022**, *179*, 401–414. [CrossRef]
37. Almqvist, H.; Pateraki, C.; Alexandri, M.; Koutinas, A.; Lidén, G. Succinic Acid Production by *Actinobacillus succinogenes* from Batch Fermentation of Mixed Sugars. *J. Ind. Microbiol. Biotechnol.* **2016**, *43*, 1117–1130. [CrossRef]
38. Lin, S.K.C.; Du, C.; Koutinas, A.; Wang, R.; Webb, C. Substrate and Product Inhibition Kinetics in Succinic Acid Production by *Actinobacillus succinogenes*. *Biochem. Eng. J.* **2008**, *41*, 128–135. [CrossRef]
39. Ferone, M.; Raganati, F.; Olivieri, G.; Salatino, P.; Marzocchella, A. Biosuccinic Acid from Lignocellulosic-Based Hexoses and Pentoses by *Actinobacillus succinogenes*: Characterization of the Conversion Process. *Appl. Biochem. Biotechnol.* **2017**, *183*, 1465–1477. [CrossRef]
40. Pateraki, C.; Almqvist, H.; Ladakis, D.; Lidén, G.; Koutinas, A.A.; Vlysidis, A. Modelling Succinic Acid Fermentation Using a Xylose Based Substrate. *Biochem. Eng. J.* **2016**, *114*, 26–41. [CrossRef]
41. Cimini, D.; Zaccariello, L.; D’Ambrosio, S.; Lama, L.; Ruoppolo, G.; Pepe, O.; Faraco, V.; Schiraldi, C. Improved Production of Succinic Acid from *Basfia succiniciproductens* Growing on A. Donax and Process Evaluation through Material Flow Analysis. *Biotechnol. Biofuels* **2019**, *12*, 22. [CrossRef]
42. Thuy, N.T.H.; Kongkaew, A.; Flood, A.; Boontawan, A. Fermentation and Crystallization of Succinic Acid from *Actinobacillus succinogenes* ATCC55618 Using Fresh Cassava Root as the Main Substrate. *Bioresour. Technol.* **2017**, *233*, 342–352. [CrossRef]
43. Briki, A.; Kaboré, K.; Olmos, E.; Bosselaar, S.; Blanchard, F.; Fick, M.; Guedon, E.; Fournier, F.; Delaunay, S. *Corynebacterium glutamicum*, a Natural Overproducer of Succinic Acid? *Eng. Life Sci.* **2020**, *20*, 205–215. [CrossRef]

44. Huang, M.; Cheng, J.; Chen, P.; Zheng, G.; Wang, D.; Hu, Y. Efficient Production of Succinic Acid in Engineered *Escherichia coli* Strains Controlled by Anaerobically-Induced NirB Promoter Using Sweet Potato Waste Hydrolysate. *J. Environ. Manag.* **2019**, *237*, 147–154. [CrossRef]
45. Filippi, K.; Papapostolou, H.; Alexandri, M.; Vlysidis, A.; Myrtsi, E.D.; Ladakis, D.; Pateraki, C.; Haroutounian, S.A.; Koutinas, A. Integrated Biorefinery Development Using Winery Waste Streams for the Production of Bacterial Cellulose, Succinic Acid and Value-Added Fractions. *Bioresour. Technol.* **2022**, *343*, 125989. [CrossRef]
46. Oreoluwa Jokodola, E.; Narisetty, V.; Castro, E.; Durgapal, S.; Coulon, F.; Sindhu, R.; Binod, P.; Rajesh Banu, J.; Kumar, G.; Kumar, V. Process Optimisation for Production and Recovery of Succinic Acid Using Xylose-Rich Hydrolysates by *Actinobacillus succinogenes*. *Bioresour. Technol.* **2022**, *344*, 126224. [CrossRef]
47. Xu, C.; Alam, M.A.; Wang, Z.; Peng, Y.; Xie, C.; Gong, W.; Yang, Q.; Huang, S.; Zhuang, W.; Xu, J. Co-Fermentation of Succinic Acid and Ethanol from Sugarcane Bagasse Based on Full Hexose and Pentose Utilization and Carbon Dioxide Reduction. *Bioresour. Technol.* **2021**, *339*, 125578. [CrossRef]
48. Ercole, A.; Raganati, F.; Salatino, P.; Marzocchella, A. Continuous Succinic Acid Production by Immobilized Cells of *Actinobacillus succinogenes* in a Fluidized Bed Reactor: Entrapment in Alginate Beads. *Biochem. Eng. J.* **2021**, *169*, 107968. [CrossRef]
49. Bradfield, M.F.A.; Mohagheghi, A.; Salvachúa, D.; Smith, H.; Black, B.A.; Dowe, N.; Beckham, G.T.; Nicol, W. Continuous Succinic Acid Production by *Actinobacillus succinogenes* on Xylose-Enriched Hydrolysate. *Biotechnol. Biofuels* **2015**, *8*, 181. [CrossRef]
50. Bradfield, M.F.A.; Nicol, W. Continuous Succinic Acid Production from Xylose by *Actinobacillus succinogenes*. *Bioprocess Biosyst. Eng.* **2016**, *39*, 233–244. [CrossRef]
51. Ferone, M.; Raganati, F.; Ercole, A.; Olivieri, G.; Salatino, P.; Marzocchella, A. Continuous Succinic Acid Fermentation by *Actinobacillus succinogenes* in a Packed-Bed Biofilm Reactor. *Biotechnol. Biofuels* **2018**, *11*, 138. [CrossRef]
52. Ferone, M.; Raganati, F.; Olivieri, G.; Marzocchella, A. Bioreactors for Succinic Acid Production Processes. *Crit. Rev. Biotechnol.* **2019**, *39*, 571–586. [CrossRef]
53. Chen, X.; Zhou, Y.; Zhang, D. Engineering *Corynebacterium crenatum* for Enhancing Succinic Acid Production. *J. Food Biochem.* **2018**, *42*, e12645. [CrossRef]
54. Ahn, J.H.; Jang, Y.S.; Lee, S.Y. Production of Succinic Acid by Metabolically Engineered Microorganisms. *Curr. Opin. Biotechnol.* **2016**, *42*, 54–66. [CrossRef] [PubMed]
55. Jiang, M.; Ma, J.; Wu, M.; Liu, R.; Liang, L.; Xin, F.; Zhang, W.; Jia, H.; Dong, W. Progress of Succinic Acid Production from Renewable Resources: Metabolic and Fermentative Strategies. *Bioresour. Technol.* **2017**, *245*, 1710–1717. [CrossRef] [PubMed]
56. Yang, Q.; Wu, M.; Dai, Z.; Xin, F.; Zhou, J.; Dong, W.; Ma, J.; Jiang, M.; Zhang, W. Comprehensive Investigation of Succinic Acid Production by *Actinobacillus succinogenes*: A Promising Native Succinic Acid Producer. *Biofuels Bioprod. Biorefining* **2019**, *14*, 950–964. [CrossRef]
57. Grossmann, I.E.; Harjunkoski, I. Process Systems Engineering: Academic and Industrial Perspectives. *Comput. Chem. Eng.* **2019**, *126*, 474–484. [CrossRef]
58. Solano-Cornejo, M.A.; Vidaurre-Ruiz, J.M. Application of Unstructured Kinetic Models in the Lactic Fermentation Modeling of the Fishery By-Products. *Sci. Agropecu.* **2017**, *8*, 367–375. [CrossRef]
59. Almquist, J.; Cvijovic, M.; Hatzimanikatis, V.; Nielsen, J.; Jirstrand, M. Kinetic Models in Industrial Biotechnology—Improving Cell Factory Performance. *Metab. Eng.* **2014**, *24*, 38–60. [CrossRef]
60. Theodoropoulos, C.; Chenhao, S. Bioreactor Models and Modeling Approaches. *Eng. Perspect. Biotechnol. Compr. Biotechnol.* **2019**, *2*, 663–680.
61. Alcón Martín, A. *Desarrollo de Modelos Cinéticos para Bioprocesos: Aplicación a la Producción de Xantano*; Complutense University: Madrid, Spain, 1999. Available online: <https://eprints.ucm.es/id/eprint/3549/> (accessed on 14 January 2022).
62. Celler, K.; Picioreanu, C.; van Loosdrecht, M.; van Wezel, G.P. Structured morphological modeling as a framework for rational strain design of *Streptomyces* species. *Antonie Van Leeuwenhoek* **2012**, *102*, 409–423. [CrossRef]
63. García-Ochoa, F.; Santos, V.E.; Alcón, A. Simulation of Xanthan Gum Production by a Chemically Structured Kinetic Model. *Math. Comput. Simul.* **1996**, *42*, 187–195. [CrossRef]
64. Quirós, C.; Herrero, M.; García, L.A.; Díaz, M. Application of Flow Cytometry to Segregated Kinetic Modeling Based on the Physiological States of Microorganisms. *Appl. Environ. Microbiol.* **2007**, *73*, 3993–4000. [CrossRef]
65. García-Ochoa, F.; Castro, E.G.; Santos, V.E. Oxygen Transfer and Uptake Rates during Xanthan Gum Production. *Enzym. Microb. Technol.* **2000**, *27*, 680–690. [CrossRef]
66. Corona-González, R.I.; Varela-Almanza, K.M.; Arriola-Guevara, E.; de Jesús Martínez-Gómez, Á.; Pelayo-Ortiz, C.; Toriz, G. Bagasse Hydrolyzates from Agave Tequilana as Substrates for Succinic Acid Production by *Actinobacillus succinogenes* in Batch and Repeated Batch Reactor. *Bioresour. Technol.* **2016**, *205*, 15–23. [CrossRef]
67. Vemuri, G.N.; Eiteman, M.A.; Altman, E. Succinate Production in Dual-Phase *Escherichia coli* Fermentations Depends on the Time of Transition from Aerobic to Anaerobic Conditions. *J. Ind. Microbiol. Biotechnol.* **2002**, *28*, 325–332. [CrossRef]
68. Litsanov, B.; Bocker, M.; Bott, M. Toward Homosuccinate Fermentation: Metabolic Engineering of *Corynebacterium glutamicum* for Anaerobic Production of Succinate from Glucose and Formate. *Appl. Environ. Microbiol.* **2012**, *78*, 3325–3337. [CrossRef]

69. Ong, K.L.; Fickers, P.; Lin, C.S.K. Enhancing Succinic Acid Productivity in the Yeast *Yarrowia lipolytica* with Improved Glycerol Uptake Rate. *Sci. Total Environ.* **2020**, *702*, 134911. [[CrossRef](#)]
70. Corona-González, R.I.; Miramontes-Murillo, R.; Arriola-Guevara, E.; Guatemala-Morales, G.; Toriz, G.; Pelayo-Ortiz, C. Immobilization of *Actinobacillus succinogenes* by Adhesion or Entrapment for the Production of Succinic Acid. *Bioresour. Technol.* **2014**, *164*, 113–118. [[CrossRef](#)]
71. Meynial-salles, I.; Dorotyn, S.; Soucaille, P. A New Process for the Continuous Production of Succinic Acid from Glucose at High Yield, Titer, and Productivity. *Biotechnol. Bioeng.* **2008**, *99*, 129–135. [[CrossRef](#)]
72. Ito, Y.; Hirasawa, T.; Shimizu, H. Metabolic Engineering of *Saccharomyces cerevisiae* to Improve Succinic Acid Production Based on Metabolic Profiling. *Biosci. Biotechnol. Biochem.* **2014**, *78*, 151–159. [[CrossRef](#)]
73. Kim, D.Y.; Yim, S.C.; Lee, P.C.; Lee, W.G.; Lee, S.Y.; Chang, H.N. Batch and Continuous Fermentation of Succinic Acid from Wood Hydrolysate by *Mannheimia succiniciproducens* MBEL55E. *Enzym. Microb. Technol.* **2004**, *35*, 648–653. [[CrossRef](#)]
74. Dessie, W.; Xin, F.; Zhang, W.; Zhou, J.; Wu, H.; Ma, J.; Jiang, M. Inhibitory Effects of Lignocellulose Pretreatment Degradation Products (Hydroxymethylfurfural and Furfural) on Succinic Acid Producing *Actinobacillus succinogenes*. *Biochem. Eng. J.* **2019**, *150*, 107263. [[CrossRef](#)]
75. Andersson, C.; Helmerius, J.; Hodge, D.; Berglund, K.; Rova, U. Inhibition of Succinic Acid Production in Metabolically Engineered *Escherichia coli* by Neutralizing Agent, Organic Acids, and Osmolarity. *Biotechnol. Prog.* **2009**, *25*, 116–123. [[CrossRef](#)]
76. Kuglarz, M.; Rom, M. Influence of Carbon Dioxide and Nitrogen Source on Sustainable Production of Succinic Acid from Miscanthus Hydrolysates. *Int. J. Environ. Sci. Dev.* **2019**, *10*, 362–367. [[CrossRef](#)]
77. Liu, Y.; Wu, H.; Li, Q.; Tang, X.; Li, Z.; Ye, Q. Enzyme and Microbial Technology Process Development of Succinic Acid Production by *Escherichia coli* NZN111 Using Acetate as an Aerobic Carbon Source. *Enzym. Microb. Technol.* **2011**, *49*, 459–464. [[CrossRef](#)] [[PubMed](#)]
78. Li, Q.; Wang, D.; Wu, Y.; Yang, M.; Li, W.; Xing, J.; Su, Z. Kinetic Evaluation of Products Inhibition to Succinic Acid Producers *Escherichia coli* NZN111, AFP111, BL21, and *Actinobacillus succinogenes* 130ZT. *J. Microbiol.* **2010**, *48*, 290–296. [[CrossRef](#)]
79. Corona-González, R.I.; Bories, A.; González-Álvarez, V.; Pelayo-Ortiz, C. Kinetic Study of Succinic Acid Production by *Actinobacillus succinogenes* ZT-130. *Process Biochem.* **2008**, *43*, 1047–1053. [[CrossRef](#)]
80. Purvis, J.E.; Yomano, L.P.; Ingram, L.O. Enhanced Trehalose Production Improves Growth of *Escherichia coli* under Osmotic Stress. *Appl. Environ. Microbiol.* **2005**, *71*, 3761–3769. [[CrossRef](#)]
81. Panikov, N.S. *Microbial Growth Kinetics*; Springer Science & Business Media: Berlin/Heidelberg, Germany, 1995.
82. Sadhukhan, S.; Villa, R.; Sarkar, U. Microbial Production of Succinic Acid Using Crude and Purified Glycerol from a *Crotalaria juncea* Based Biorefinery. *Biotechnol. Rep.* **2016**, *10*, 84–93. [[CrossRef](#)]
83. Song, H.; Jang, S.H.; Park, J.M.; Lee, S.Y. Modeling of Batch Fermentation Kinetics for Succinic Acid Production by *Mannheimia succiniciproducens*. *Biochem. Eng. J.* **2008**, *40*, 107–115. [[CrossRef](#)]
84. Luong, J.H.T.; Mulchandani, A. Microbial Inhibition Kinetics Revisited. *Enzym. Microb. Technol.* **1989**, *11*, 66–73.
85. Brink, H.G.; Nicol, W. Succinic Acid Production with *Actinobacillus succinogenes*: Rate and Yield Analysis of Chemostat and Biofilm Cultures. *Microb. Cell Fact.* **2014**, *13*, 111. [[CrossRef](#)]
86. Vlysidis, A.; Binns, M.; Webb, C.; Theodoropoulos, C. Glycerol Utilisation for the Production of Chemicals: Conversion to Succinic Acid, a Combined Experimental and Computational Study. *Biochem. Eng. J.* **2011**, *58–59*, 1–11. [[CrossRef](#)]
87. Carvalho, M.; Roca, C.; Reis, M.A.M. Improving Succinic Acid Production by *Actinobacillus succinogenes* from Raw Industrial Carob Pods. *Bioresour. Technol.* **2016**, *218*, 491–497. [[CrossRef](#)]
88. Carvalho, M.; Roca, C.; Reis, M.A.M. Carob Pod Water Extracts as Feedstock for Succinic Acid Production by *Actinobacillus succinogenes* 130Z. *Bioresour. Technol.* **2014**, *170*, 491–498. [[CrossRef](#)]
89. Luthfi, A.A.I.; Jahim, J.M.; Harun, S.; Tan, J.P.; Manaf, S.F.A.; Shah, S.S.M. Kinetics of the Bioproduction of Succinic Acid by *Actinobacillus succinogenes* from Oil Palm Lignocellulosic Hydrolysate in a Bioreactor. *BioResources* **2018**, *13*, 8279–8294. [[CrossRef](#)]
90. Ferone, M.; Raganati, F.; Olivieri, G.; Salatino, P.; Marzocchella, A. Continuous Succinic Acid Fermentation by *Actinobacillus succinogenes*: Assessment of Growth and Succinic Acid Production Kinetics. *Appl. Biochem. Biotechnol.* **2019**, *187*, 782–799. [[CrossRef](#)]
91. Li, C.; Xiao, Y.; Sang, Z.; Yang, Z.; Xu, T.; Yang, X.; Yan, J.; Lin, C.S.K. Inhibition Kinetics of Bio-Based Succinic Acid Production by the Yeast *Yarrowia lipolytica*. *Chem. Eng. J.* **2022**, *442*, 136273. [[CrossRef](#)]
92. Garcia-Ochoa, F.; Gomez, E. Bioreactor Scale-up and Oxygen Transfer Rate in Microbial Processes: An Overview. *Biotechnol. Adv.* **2009**, *27*, 153–176. [[CrossRef](#)]
93. Silva, E.M.; Yang, S.T. Kinetics and Stability of a Fibrous-Bed Bioreactor for Continuous Production of Lactic Acid from Unsupplemented Acid Whey. *J. Biotechnol.* **1995**, *41*, 59–70. [[CrossRef](#)]
94. Richelle, A. Modelling, Optimization and Control of Yeast Fermentation Processes in Food Industry. Ph.D. Thesis, Université Libre de Bruxelles, Brussels, Belgium, 2014. [[CrossRef](#)]
95. Kumar, A.; Ray, D.K.; Gupta, S.M. Bioprocess Technology. In *Biotechnology in Medicine and Agriculture: Principles and Practices*; International Publishing House: New York, NY, USA, 2012; pp. 827–857.
96. Yasin, M.; Jang, N.; Lee, M.; Kang, H.; Aslam, M.; Bazmi, A.A.; Chang, I.S. Bioreactors, Gas Delivery Systems and Supporting Technologies for Microbial Synthesis Gas Conversion Process. *Bioresour. Technol. Rep.* **2019**, *7*, 100207. [[CrossRef](#)]

97. Escobar, S.; Rodriguez, A.; Gomez, E.; Alcon, A.; Santos, V.E.; Garcia-Ochoa, F. Influence of Oxygen Transfer on *Pseudomonas putida* Effects on Growth Rate and Biodesulfurization Capacity. *Bioprocess. Biosyst. Eng.* **2016**, *39*, 545–554. [[CrossRef](#)]
98. Xi, Y.; Chen, K.; Li, J.; Fang, X.; Zheng, X.; Sui, S.; Jiang, M.; Wei, P. Optimization of Culture Conditions in CO₂ Fixation for Succinic Acid Production Using *Actinobacillus succinogenes*. *J. Ind. Microb. Biotechnol.* **2011**, *38*, 1605. [[CrossRef](#)] [[PubMed](#)]
99. Herselman, J.; Bradfield, M.F.A.; Vijayan, U.; Nicol, W. The Effect of Carbon Dioxide Availability on Succinic Acid Production with Biofilms of *Actinobacillus succinogenes*. *Biochem. Eng. J.* **2017**, *117*, 218–225. [[CrossRef](#)]
100. Villadsen, J.; Nielsen, J.; Lidén, G. *Bioreaction Engineering Principles*; Springer: Berlin/Heidelberg, Germany, 2011; ISBN 9788578110796.
101. Elhajj, J.; Al-Hindi, M.; Azizi, F. A Review of the Absorption and Desorption Processes of Carbon Dioxide in Water Systems. *Ind. Eng. Chem. Res.* **2014**, *53*, 2–22. [[CrossRef](#)]
102. Liu, Y.P.; Zheng, P.; Sun, Z.H.; Ni, Y.; Dong, J.J.; Wei, P. Strategies of PH Control and Glucose-Fed Batch Fermentation for Production of Succinic Acid by *Actinobacillus succinogenes*. *J. Chem. Technol. Biotechnol.* **2008**, *83*, 1163–1169. [[CrossRef](#)]
103. Cao, W.; Wang, Y.; Luo, J.; Yin, J.; Xing, J.; Wan, Y. Effectively Converting Carbon Dioxide into Succinic Acid under Mild Pressure with *Actinobacillus succinogenes* by an Integrated Fermentation and Membrane Separation Process. *Bioresour. Technol.* **2018**, *266*, 26–33. [[CrossRef](#)]
104. Wu, M.; Zhang, W.; Ji, Y.; Yi, X.; Ma, J.; Wu, H.; Jiang, M. Coupled CO₂ Fixation from Ethylene Oxide Off-Gas with Bio-Based Succinic Acid Production by Engineered Recombinant *Escherichia coli*. *Biochem. Eng. J.* **2017**, *117*, 1–6. [[CrossRef](#)]
105. Song, H.; Lee, J.W.; Choi, S.; You, J.K.; Hong, W.H.; Lee, S.Y. Effects of Dissolved CO₂ Levels on the Growth of *Mannheimia succiniciproducens* and Succinic Acid Production. *Biotechnol. Bioeng.* **2007**, *98*, 1296–1304. [[CrossRef](#)]
106. Zou, W.; Zhu, L.-W.; Li, H.-M.; Tang, Y.-J. Significance of CO₂ Donor on the Production of Succinic Acid by *Actinobacillus succinogenes* ATCC 55618. *Microb. Cell Fact.* **2011**, *10*, 87. [[CrossRef](#)]
107. Gunnarsson, I.B.; Alvarado-Morales, M.; Angelidaki, I. Utilization of CO₂ Fixating Bacterium *Actinobacillus succinogenes* 130Z for Simultaneous Biogas Upgrading and Biosuccinic Acid Production. *Environ. Sci. Technol.* **2014**, *48*, 12464–12468. [[CrossRef](#)]
108. Amulya, K.; Kopperi, H.; Venkata Mohan, S. Tunable Production of Succinic Acid at Elevated Pressures of CO₂ in a High Pressure Gas Fermentation Reactor. *Bioresour. Technol.* **2020**, *309*, 123327. [[CrossRef](#)]
109. Schumpe, A.; Deckwer, W.D. Estimation of O₂ and CO₂ Solubilities in Fermentation Media. *Biotechnol. Bioeng.* **1979**, *21*, 298–300. [[CrossRef](#)]
110. Weisenberger, S.; Schumpe, A. Estimation of Gas Solubilities in Salt Solutions at Temperatures from 273 K to 363 K. *AIChE J.* **1996**, *42*, 298–300. [[CrossRef](#)]
111. Rischbieter, E.; Schumpe, A.; Wunder, V. Gas Solubilities in Aqueous Solutions of Organic Substances. *J. Chem. Eng. Data* **1996**, *41*, 809–812. [[CrossRef](#)]
112. Pitault, I.; Fongarland, P.; Koepke, D.; Mitrovic, M.; Ronze, D.; Forissier, M. Gas–Liquid and Liquid–Solid Mass Transfers in Two Types of Stationary Catalytic Basket Laboratory Reactor. *Chem. Eng. Sci.* **2005**, *60*, 6240–6253. [[CrossRef](#)]
113. Royce, P.N. Effect of Changes in the pH and Carbon Dioxide Evolution Rate on the Measured Respiratory Quotient of Fermentations. *Biotechnol. Bioeng.* **1992**, *40*, 1129–1138. [[CrossRef](#)]
114. Rigaki, A.; Webb, C.; Theodoropoulos, C. Double Substrate Limitation Model for the Bio-Based Production of Succinic Acid from Glycerol. *Biochem. Eng. J.* **2020**, *153*, 107391. [[CrossRef](#)]
115. Hill, G.A. Measurement of Overall Volumetric Mass Transfer Coefficients for Carbon Dioxide in a Well-Mixed Reactor Using a pH Probe. *Ind. Eng. Chem. Res.* **2006**, *45*, 5796–5800. [[CrossRef](#)]
116. Kordač, M.; Linek, V. Dynamic Measurement of Carbon Dioxide Volumetric Mass Transfer Coefficient in a Well-Mixed Reactor Using a pH Probe: Analysis of the Salt and Supersaturation Effects. *Ind. Eng. Chem. Res.* **2008**, *47*, 1310–1317. [[CrossRef](#)]
117. Longanesi, L.; Frascari, D.; Spagni, C.; DeWever, H.; Pinelli, D. Succinic Acid Production from Cheese Whey by Biofilms of *Actinobacillus succinogenes*: Packed Bed Bioreactor Tests. *J. Chem. Technol. Biotechnol.* **2018**, *93*, 246–256. [[CrossRef](#)]
118. Kim, S.Y.; Park, S.O.; Yeon, J.Y.; Chun, G.T. Development of a Cell-Recycled Continuous Fermentation Process for Enhanced Production of Succinic Acid by High-Yielding Mutants of *Actinobacillus succinogenes*. *Biotechnol. Bioprocess Eng.* **2021**, *26*, 125–136. [[CrossRef](#)]
119. Mokwatlo, S.C.; Nchabeleng, M.E.; Brink, H.G.; Nicol, W. Impact of Metabolite Accumulation on the Structure, Viability and Development of Succinic Acid-Producing Biofilms of *Actinobacillus succinogenes*. *Appl. Microbiol. Biotechnol.* **2019**, *103*, 6205–6215. [[CrossRef](#)] [[PubMed](#)]
120. Mokwatlo, S.C.; Brink, H.G.; Nicol, W. Effect of Shear on Morphology, Viability and Metabolic Activity of Succinic Acid-Producing *Actinobacillus succinogenes* Biofilms. *Bioprocess Biosyst. Eng.* **2020**, *43*, 1253–1263. [[CrossRef](#)] [[PubMed](#)]
121. Mokwatlo, S.C.; Nicol, W. Structure and Cell Viability Analysis of *Actinobacillus succinogenes* Biofilms as Biocatalysts for Succinic Acid Production. *Biochem. Eng. J.* **2017**, *128*, 134–140. [[CrossRef](#)]
122. Beyenal, H.; Tanyolaç, A.; Lewandowski, Z. Measurement of Local Effective Diffusivity in Heterogeneous Biofilms. *Water Sci. Technol.* **1998**, *38*, 171–178. [[CrossRef](#)]
123. Beyenal, H.; Lewandowski, Z. Combined Effect of Substrate Concentration and Flow Velocity on Effective Diffusivity in Biofilms. *Water Res.* **2000**, *34*, 528–538. [[CrossRef](#)]
124. Mokwatlo, S.C.; Nicol, W.; Brink, H.G. Internal Mass Transfer Considerations in Biofilms of Succinic Acid Producing *Actinobacillus succinogenes*. *Chem. Eng. J.* **2021**, *407*, 127220. [[CrossRef](#)]

125. Horn, H.; Hempel, D.C. Substrate Utilization and Mass Transfer in an Autotrophic Biofilm System: Experimental Results and Numerical Simulation. *Biotechnol. Bioeng.* **1997**, *53*, 363–371. [[CrossRef](#)]
126. Wäsche, S.; Horn, H.; Hempel, D.C. Influence of Growth Conditions on Biofilm Development and Mass Transfer at the Bulk/Biofilm Interface. *Water Res.* **2002**, *36*, 4775–4784. [[CrossRef](#)]
127. Galaction, A.-I.; Rotaru, R.; Kloetzer, L.; Vlysidis, A.; Webb, C.; Turnea, M.; Cascaval, D. External and Internal Glucose Mass Transfers in Succinic Acid Fermentation with Stirred Bed of Immobilized *Actinobacillus succinogenes* under Substrate and Product Inhibitions. *J. Microbiol. Biotechnol.* **2011**, *21*, 1257–1263. [[CrossRef](#)]
128. Galaction, A.-I.; Kloetzer, L.; Turnea, M.; Webb, C.; Vlysidis, A.; Cașcaval, D. Succinic Acid Fermentation in a Stationary-Basket Bioreactor with a Packed Bed of Immobilized *Actinobacillus succinogenes*: 1. Influence of Internal Diffusion on Substrate Mass Transfer and Consumption Rate. *J. Ind. Microbiol. Biotechnol.* **2012**, *39*, 877–888. [[CrossRef](#)]